Correlation between the kinematics of a Tunnel Boring Machine and the observed soil displacements

Broere, W.; Festa, D.

DOI
10.1016/j.tust.2017.07.014

Publication date
2017

Document Version
Accepted author manuscript

Published in
Tunnelling and Underground Space Technology

Postprint of Tunnelling and Underground Space Technology
Volume 70, November 2017, Pages 125-147
Link to formal publication (Elsevier): https://doi.org/10.1016/S1001-6058(16)60755-2

Correlation between the kinematics of a Tunnel Boring Machine and the observed soil displacements

W. Broere[1], D. Festa[2]

(1) Delft University of Technology, Faculty of Civil Engineering and Geosciences, Department of Geoscience and Engineering, Geo-Engineering Section, Delft, The Netherlands

(2) Royal HaskoningDHV, Amersfoort, The Netherlands

Corresponding author: W. Broere, Stevinweg 1, 2628 CN Delft, The Netherlands; w.broere@tudelft.nl, Ph. +31 (0)15 27 81545

Keywords: Soft-soil tunnelling, TBM kinematics, subsurface displacements, monitoring

Abstract

Constructing tunnels in soft soil with the use of Tunnel Boring Machines (TBMs) may induce settlements. A considerable amount of the total soil displacements is correlated with the passage of the TBM-shield. Even so, the TBM-induced soil displacements are so far only coarsely correlated to the total settlements. This paper relates the shield geometry and its advance through the soil with the observed soil displacements. The snake-like motion of the shield induces unevenly distributed soil displacements at the shield-soil interface, which spread through the soil with a similar pattern. The results of an earlier numerical investigation on the TBM kinematics and the observed soil response are compared here in order to quantify their correlation. The analysis has been based on the monitoring data from the construction of a twin-tube bored road tunnel in The Hague, The Netherlands. Results confirm that the geometry and the advance of the TBM-shield through the soil influence the amount and distribution of the induced soil displacements. The analysis also highlights the essential role of the tail-void grouting not only in filling-in the tail-void, but also in compensating the kinematical effects of shield advance.

1 Introduction

Tunnel Boring Machines (TBMs) are increasingly used to construct tunnels in built-up environments. As a construction technique, it proved effective and socially acceptable (Lance and Anderson, 2006). Nevertheless, stricter standards are progressively set on design engineers, TBM manufacturers, and operators. Predicting how the tunnel construction will affect its surroundings is one of the major concerns. Unfortunately, the current soil-settlement predictions are still largely based on the experience gained from previous projects, therefore often lacking in adequate case-specificity (Mair and Taylor, 1997). In other words, the expected level of risk is defined through the volume loss concept, as obtained from previous tunnelling experiences in similar circumstances. The volume loss allows then to derive the expected movements of the surrounding soil and constructions as it is processed via empirical (Peck, 1969; Vu et al. 2015), analytical (Verruijt, 1997), or numerical analyses (Sugimoto and Sramoon, 2002; Komiya et al. 1999; Sugimoto et al., 2007; Nagel, 2009; Mair et al. 1993; Mair and Taylor, 1993).

According to the volume-loss based approach, settlement predictions are hardly correlated with project-specific aspects such as the TBM features and its real kinematic behaviour when driven through the soil. Consequently, the predictions' accuracy and their reliability are negatively affected. As Mair and Burland (1996), Mair and Taylor (1999) and Vu et al. (2016) discuss, the observed volume loss is made up of contributions due to soil relaxation and movements ahead of the TBM face, due to the shape, tapering and overcut of the TBM, due to the interaction between soil and process fluids such as bentonite suspension and grout injected at the tail, and due to relaxation, consolidation and creep of the soil after the TBM has passed. Of these aspects, the interaction processes between the TBM, the soil, and the process fluids certainly represent a critical aspect. Their better understanding can improve the reliability of the overall tunnel boring process.

The disregard concerning the consequences of the TBM's features and its operation is particularly surprising considering that the longitudinal settlement profiles often show the significant effect of the

shield transit on the overall induced surface settlements. This has been shown, among others, by the shield-soil interaction models by Sugimoto and Sramoon (2002), Standing and Selemetas (2013), Kasper and Meschke (2006), and Nagel et al. (2010). The snake-like motion of the shield within the excavated soil profile is one of the key aspects highlighted by Sugimoto and Sramoon (2002).

The current study aims to establish a quantitative correlation between the soil displacements observed during the construction of a TBM-driven tunnel and the specific driving pattern of the TBM (Festa et al., 2013, 2015). In particular, the correlation is investigated between the TBM-shield interaction with the trajectory excavated by the cutting wheel and the soil response as measured through inclinometers and extensometers. The study is based on the monitoring-data collected during the construction of the Hubertus tunnel, as for this project both TBM data and soil-displacement monitoring data were available.

2 Hubertus Tunnel

The Hubertus tunnel is a twin-tube road tunnel located in The Hague, The Netherlands, excavated between 2006 and 2007. Situated in a residential area, the tunnel passes close to the foundations of some houses and in part underpasses several low buildings on a military barracks.The two tunnel tubes, north and south, are 1496.81 m and 1483.59 m long, respectively (Festa et al, 2012).

The tubes were excavated by a non-articulated 10 680 mm long Herrenknecht Hydroshield TBM shown in Fig. 1. The shield had a front diameter of 10 510 mm, and a rear one of 10 490 mm (i.e. with a radial tapering of 10 mm). A permanent radial overcutting of 10 mm was used. The cutting wheel, supported by a longitudinally displaceable spherical bearing, was handled via three couples of hydraulic cylinders. The tail-void was grouted via the upper four of the six injection openings available at the shield tail. The final lining is formed by 2 m long prefab reinforced-concrete elements, with an external diameter of 10 200 mm. The theoretical tail-void gap was 145 mm.

The sharpest horizontal curve, with a curvature radius of 542.3 m, is located in the southern alignment, and was bored in leftward direction. The deepest point of the tunnel axis is located 27.73 m below surface. The groundwater level is assumed with sufficient accuracy at +1.0 m above N.A.P. (Dutch Reference System approximately equivalent to the Mean Sea Level). A reference stratigraphic profile of the Hubertus tunnel is provided in Figure 2. The profile crossed by the tunnel consisted of sands and silty sands with variable densities, and few clay and silt lenses. A modest clay layer not thicker than 1 m was encountered in the deepest tunnelling sector (unit 13 in Fig. 2). A peat layer of about 1.5 m was present approximately between NAP +1.50 and +0.00 m, but not crossed by the tunnel. The tunnel was in fact entirely bored through Holocene soil layers, as the limit between the Holocene and the Pleistocene formations is lying around NAP -22.0 m at this location. Table 1 gives an overview of the classification of the various soil layers and some characteristic parameters.

During tunnel construction, subsurface displacements were monitored by 4 cross-sections equipped with extensometers paired with 4 cross-sections with inclinometers. In the plan view of Fig. 2, four cross-sections indicate the approximate locations where extensometers and inclinometers were installed. The exact locations of the cross-sections are provided in Tables 2 and 3 with reference to the tunnel advance. The horizontal distance between two matching monitoring sections (for inclinometers and extensometers) was around 1.2 m. The location of the monitoring sections expressed in terms of tunnel advance differed between the two tubes. That was due to an overall difference in length of about 13 m between the two tubes.

Each monitoring section was equipped with 7 boreholes. In the boreholes either extensometers or inclinometers were installed. The boreholes were numbered from 1 to 7 from right towards left, as seen in direction of drive. Only 5 of the 7 boreholes were actually instrumented during each passage of the shield. Those were chosen as the closest ones with respect to the tunnel being bored at that time. For each cross-section the time span investigated ranged from the moment in which the TBM-face was 25 m before the section (whenever the completeness of the monitoring data allowed that), until the face was 50 m after the section. These positions are depicted in Figs. 4 to 15 as -25 and +50, respectively. See Fig. 3 for a graphical explanation.

2.1 Extensometers

Extensometers were used at the Hubertus tunnel to monitor the underground vertical displacements, with conventional levelling used to monitor the vertical movements of the surface reference point. The movements logged at the four monitoring sections equipped with extensometers are plotted in Figs. 4 to 11, for both the south and north tubes.

Each graph refers to one sensor and the cross symbol next to the graph indicates the depth of the sensor. The zero settlement reference value was assumed with the shield face 25 m before the monitoring section. Data was collected continuously during advance. The only exception occurred at the first passage across section 1. There data logging was not started in time and the reference point was taken with the shield face only 10 m before the section. Vertical lines mark meaningful relative positions of the TBM-shield face with respect to the monitoring section. For instance, the line corresponding to 0 represents the moment in which the cutter face crosses the monitoring section. The line corresponding to +10.235 stands for the transit of the shield tail across the monitoring section.

Moreover, a more traditional description of the tunnelling induced settlements is provided through the same figures. The progress of the settlement troughs at different depths is represented. For simplicity, settlement troughs for a selected number of advances only were drawn.

During the first passage of the TBM across the first cross-section (Fig. 4) a maximum observed settlement of 35 mm occurs on the centre line directly above the TBM, and results in slightly lower surface settlements. Approximately 0.5D to the left of the TBM (or 1D from the centre line) maximum surface and subsurface settlements of 10 mm occur, whereas 0.5D to the right the maximum settlements amount to 5 mm. During the second TBM passage (Fig. 5) the maximum deformation during TBM passage amounted to 20 mm at the centre line, with a strong recovery at the tail. This resulted in final surface settlements of 15 mm along the centre line, and only 5 mm remaining deformation close to the tunnel. At the left side, 0.5D from the TBM side, 5 mm of maximum settlement is recorded, whereas on the other side 4 mm of initial settlement is completely recovered during tail passage.

It shows the settlement troughs resulting from the tunnel construction were non-symmetrical with respect to the tunnel axis (Figs. 4 and 5). This applies to both crossings. In particular, the settlements were larger at the left-hand side than at the right-hand one.

Also, a marked and sudden recovery (heave) of the prior settlements was observed, during the second passage (Fig. 5), a few metres before the shield tail crossed the monitoring section. A similar recovery was not present during the first passage (Fig. 4). It is also noticeable that the heave was more effective close to the tunnel, and especially just above it, than at distance. For instance, considering borehole 3 above the second tunnel axis (Fig. 5), about 75% of the prior settlements were recovered at the depth of the deepest sensor (located 2 m above the extrados of the tunnel), while only 25% was recovered at surface.

The soil response during the crossing of the second monitoring section (Figs 6 and 7) showed analogies with that observed during the crossing of the first one. The non-symmetrical character of the vertical displacements was still present although less pronounced here. Settlements at the left-hand side of the tunnel under construction were larger than at the right-hand one. Maximum settlements at the centre line of 13 mm were recorded, during first passage, with a slight reduction after the tail passed. In addition, the prior soil settlements were more effectively recovered close to the tunnel than at distance. That was particularly well visible at boreholes 5 and 3 at first (Fig. 6) and second (Fig. 7) passage, respectively. At the level of the deepest sensors the downward trend was reversed when the shield face was between +5 to +10.235 m past the monitoring section.

Surface and subsurface settlements remained less than 5 mm in the cross sections 0.5D out from the TBM and were essentially 0 at distances more than 1D out from the TBM.

At the crossing of the third monitoring section some peculiarities observed earlier were confirmed, but also anomalies appeared. The effectiveness of the settlement recovery above the tunnel alignments was captured in boreholes 5 and 3 during the first (Fig. 8) and the second (Fig. 9) passage, respectively. Surface settlements were limited to 5mm during the first passage, although subsurface settlements of 10 mm were recorded. Unusual settlements were recorded by sensors 2 and 3 in borehole 6 during the first crossing (Fig. 8). During the same crossing the vertical movements in borehole 4 were also quite contrasted in direction, although limited in magnitude. From top to bottom along borehole 4 the displacements changed from 5mm downward, to neutral, to 5mm upward, to

downward again. The physical meaning of this soil response will be discussed later. Also interesting were the soil movements signalled by boreholes 1 and 2 during the second crossing (Fig. 9). In particular both boreholes indicated soil settlement at the depth interval of sensors 1 to 3 and at ground level, and neutral or even upward movement at greater depths. Surface settlements up to 10 mm were observed, with subsurface settlements up to 20 mm occurring along the centre line. The response of boreholes 1 and 2 will be commented further in the context of the discussion of the horizontal displacements. The response of sensor 5 (-12.80 m) in BH1 (Fig. 9) was considered a reading error, as it shows a sudden downward displacement that is not matched by the sensors above and below it.

The vertical displacements observed during the crossing of the fourth monitoring section were more modest than observed at the other locations. Surface settlements were limited to 5 mm. During the first crossing (Fig. 10) no recovery of the modest prior settlements took place (BH5). During the same crossing the only interesting location was BH4. Here subsurface settlements up to 10 mm were recorded (0.5D from the right side of the TBM), which were markedly larger than the deformations at the centre line or the opposite side of the TBM. The settlement pattern there may be compared to that observed at locations 1 and 2 (BH1 and BH2) during the second crossing of cross-section 3 (Fig. 9). During the second crossing of cross-section 4 (Fig. 11) the region of major interest is the one closest to the tunnel under construction. A fairly symmetrical soil response was observed there, as from the comparison between BH2 and BH4. The settlements along those boreholes ranged from zero at ground level, to -5 to -10 mm around 4 m above the tunnel crown, to neutral again at the depth of the crown, to positive (+5 mm) around the upper half of the tunnel, and then progressively neutral again at greater depths. In BH3, above the tunnel alignment, the inverse behaviour was registered in the deepest and second deepest sensors.

The displacement patterns shown here originate from four cross-sections over a 1.5 km long tunnel alignment. The number of cross-sections monitored compared to the tunnel length is disproportionately low and may not have captured all trends of soil response during TBM advance and tunnel construction. However, the observed behavior was useful for establishing a correlation between the soil response and TBM operations.

The vertical displacement fields presented here are in line with observations by Standing and Selemetas (2013). Their referred work shows that the heave induced by the face support pressure is localized and dissipates quickly with distance. A similar soil response is observed here whenever prior settlements are recovered due to face pressures or grouting.

2.2 Inclinometers

The results of inclinometers' readings at the first monitoring section during the first and second passage (south and north) are summarized in Fig. 12. The initial reference value was usually taken with the shield face 25 m before cross-section 1. However, at the first passage the data logging suffered a delay and the reference point was taken with the shield face only 10 m before section 1. The colours distinguish the progress of the horizontal displacements as the machine approached, crossed, and left the control section.

During the first passage the soil at the left-hand side of the tunnel converged horizontally. The maximum convergence of 17 mm was observed at the depth of the first sensor in borehole 6, which was the first borehole at the left-hand side of the southern tube (Fig. 12). In borehole 7, about 3 m further left, a horizontal convergence of 8 mm was also observed at surface level. Deeper on the same side of the tunnel the observed converging displacements were 10 mm in borehole 6 and 5 mm in borehole 7. At the right-hand side, the horizontal displacements ranged from -2 mm (convergence) to +2 mm (divergence) in the sector of borehole 4 next to the tunnel, and up to -7 mm near surface (convergence). The rate of horizontal displacements observed during the actual crossing of the TBM body was limited. Actually, the movements observed from +10.235 m onwards, were presumably effects of the tail void grout consolidation and of the tunnel lining deformation. As consequence of the shield transit only a convergence of about 5 mm was observed in BH 6 (left-hand side of the tunnel) and a divergence of 2 mm in BH4 (right-hand side of the tunnel). The horizontal displacements of Figure 12 were in good agreement with the vertical ones of Figure 4. In this respect the soil relaxation at the tunnel left-hand side (BH6) was appreciable both vertically and horizontally. On the other hand both the soil settlement and horizontal convergence appeared well confined at the right-hand side (BH4).

During the second passage (Fig. 12) at the right-hand side of the tunnel the soil diverged horizontally. The diverging behaviour follows a converging phase having its peak when the TBM was mid-way past the borehole (+5 m line). The maximum rightward displacement amounted to 14 mm, and was measured at a horizontal distance of 2 m from the tunnel (BH2). At another 2.44 m further in the same direction (BH1), the displacement decreased to 12 mm. In boreholes 1 and 2 the displacements started to diverge markedly from the passage of the shield tail onward. The peak was reached when the TBM-face was 25 m past the cross-section. At the left-hand side (BH4), neither a clear convergence nor a divergence were observed at the depth of the tunnel-axis. In the same borehole a converging displacement of 5 mm was observed closer to the surface. The overall fluctuation of the horizontal displacements showed much smaller at the left-hand side than at the right-hand one. The fluctuation was limited to 5 mm in the first case, while it amounted to 20 mm in the second. It would be tempting attributing this difference to the presence of the already constructed tunnel at the left-hand side. However, similar differences were observed also during the first tunnel passage, where no neighbouring tunnel existed. The same correlation between horizontal and vertical soil displacements highlighted at the first crossing was found here. Some soil relaxation occurred at the left-hand side, with vertical displacements but limited horizontal convergence. At the right-hand side, the prior vertical displacements and horizontal convergence were recovered between +5 and +10.235 m. That was well visible in BH2 and also in BH3 above the tunnel axis.

As for the vertical displacements, also the horizontal displacements induced by the crossing of cross-section 2 (Fig. 13) were more limited than at cross-section 1 (Fig. 12). This was in accordance with the learning process which the tunnel drivers usually go through when starting the construction of a new tunnel. During the first crossing there was appreciable correlation between the recovery of the vertical movements in boreholes 4 and 5 (BH4 and BH5, Fig 13) and the recovery of the horizontal displacements in BH4. The recovery occurred between +5 and +10.235 m, therefore before the shield tail crossed the monitoring section. The horizontal recovery at the right-hand side was about 5 mm. At the left-hand side that was limited to 2 mm. The soil response to the second crossing of section 2 matched qualitatively well that of the first crossing. However, the horizontal divergence was slightly more pronounced at both sides during the second crossing than during the first one.

During the first passage of the TBM-shield through cross-section 3 (Fig. 14) horizontal divergence occurred between 0 and +10.235 m. The divergence was slightly more pronounced at the right-hand side and was in the order of 5 mm. Some recovery of the vertical settlements was observed in boreholes BH4, BH5 and BH6 in Figure 7. That recovery was matched pretty well by the modest horizontal diverging trend in BH4 and BH6 (Fig. 14 – first crossing). The measurement of horizontal movements in BH2 during the second crossing appeared unusual. The inclinometer indicated pronounced horizontal movements with the shield face still 10 to 15 m in front of the monitoring section. That appeared hardly correlated with the process of shield advance. However, the movements in BH1 showed the same trend as in BH2, that holding for both vertical and horizontal directions. This made the observed soil behaviour more problematic and not explainable with the TBM data available only. The horizontal divergence at the left-hand side during the second crossing was slightly smaller than during the first one. That could be paired with a better recovery of the vertical settlements during the first crossing than during the second one.

During the first crossing of cross-section 4 no recovery of the (modest) prior vertical displacements occurred (Fig. 15). Horizontally, that could be paired with the observation that during the same crossing no divergence was recorded between 0 and +10.235 m. The registered horizontal movements occurred either before the shield face or behind the shield tail, and were therefore not correlated with the shield kinematic advance. On the contrary, during the second crossing there was evidence of horizontal expansion between +5 and +10.235 m, particularly pronounced at the right-hand side. That enlargement matched the uplift of the extensometer sensors at depth -9.80 m (BH2 and BH4 in Figure 11). The uplift measured at -9.80 m was almost absent at -6.88 m and even inversed in sign (settlement) at -1.73 m. Likewise, the region affected by horizontal divergence was limited and corresponded approximately with the tunnel height. Above that, the disturbance dissipated quickly. This fact may qualitatively explain how sign inversion can be present in a single borehole, measurement errors aside. We may distinguish between a global effect of tunnel construction and a local effect due to more detailed advance operations of the TBM. An example is provided by the vertical displacements during the second crossing of section 4. Comparing three settlement troughs at +2.19 m, -1.73 m and -6.88 m, a concavity change appears. The settlement trough at -6.88 m had a upward oriented concavity (hogging) whereas those at -1.76 and +2.19 m had it downward (sagging). That means that the physical process that induced the concavity change did not propagate far from

the tunnel. Moreover, while local change to the soil deformation path is possible, a global inversion or recovery of all the prior movements is hard to achieve.

The subsurface horizontal soil displacement fields described in this section are well in line with those presented in Standing and Selemetas (2013). The two works seemed to converge on two points. First, the horizontal tunnelling induced soil displacements can show asymmetry between opposites sides. Second, expansive behaviours (compressive strains) tend to dissipate very quickly through the soil at increasing distance from the tunnel.

3 Kinematical interaction between a TBM-shield and the surrounding soil

The trajectory excavated by the cutter head was established by Festa et al. (2015) in a model based on the data measured during TBM operation and the physical interaction between a TBM and the surrounding soil. During TBM advance, the machine goes through an almost infinite number of configurations of static equilibrium in which the forces and the moments of forces acting on the machine are in balance. The forces on the TBM can be separated into active and passive forces. Here the active forces are the complex of operations that the machine driver controls in order to steer the TBM along the pre-defined alignment. Examples are the advance/thrust cylinders, the face support pressure, the tail void grouting pressure and volume, the displacement force on the cutter head. The passive forces represent the reaction of the surrounding soil to the displacements induced as consequence of the TBM advance. The soil frequently undergoes compression and extension, and does not remain in its original stress-strain state. The resulting soil reaction has to be accounted for in the shield equilibrium. A detailed study of the active forces was presented in Festa et al. (2012). The passive forces, derived from the kinematic behaviour of the TBM, resulting in a displacement pattern at the shield-soil interface, were introduced in Festa et al. (2015). The current paper attempts to further validate the results of the kinematical analysis in Festa et al. (2015) using the various field observations made during the construction of the Hubertus tunnel.

In this analysis the interaction between a TBM-shield and the surrounding soil will be referred to as shield-soil interface displacement. The interface displacements can be quantified by accounting for the relative distance between the shield-skin at any tunnel advance and the excavated profile. The shield may be in direct contact with the soil or a gap filled with bentonite slurry or grout may exist in between (Bezuijen, 2007). A simplified version of this interaction is represented in Fig. 16a. At the left-hand side of the rectangle representing a horizontal cross-section of the shield, the surrounding soil is compressed along the first half of the length, and relaxed in the second half. The opposite is true at the right-hand side. Conventionally, compressions and extensions are represented with the negative and positive sign, respectively. The two graphs of Fig. 16b represent the progress of the interface displacements along the shield. Both interaction lines start from the origin of the axes, and that is because at the shield face, the side of the shield and excavated profiles are coincident.

The deviation of the TBM-shield from the planned tunnel alignments was thoroughly investigated in a previous study by Festa et al. (2015). That investigation aimed at studying the TBM's kinematic behaviour with respect to the surrounding soil as derived from the observed TBM positioning data at the Hubertus tunnel. The research method consisted of comparing the actual consecutive positions of the shield with the excavated soil profile, i.e. the cavity excavated by the cutter head through the soil. The excavated profile was in turn obtained as the record of the positions incrementally occupied by the cutter head as the TBM advanced. By comparing the spatial position of the TBM's shield and the geometry of the excavated cavity, the displacements induced by the advancing shield at the shield-soil interface can be quantified. The original purpose-built numerical model, introduced in Festa et al. (2011) and extended in Festa et al. (2015), was implemented in MATLAB. The deviations of the TBM from the planned south and north tunnel alignment are summarized in Fig. 17. The x-axis represents the tunnel advance and uses the same local coordinate system as in Fig. 1, where -1660.088 m corresponds to the start of tunnel-boring and -169.891 m marks its end (both advances refer to the main tunnel alignment). For both tubes the vertical deviation from the planned alignment amounts to 50 mm, whereas an incidental maximum horizontal deviation of 90 mm occurs. These are exceptions and normally the TBM closely follows the planned alignment with swings between +10mm and -10mm of the planned alignment.

Given this observed sideways moving or snaking motion of the TBM (Fig. 17), it is reasonable to expect sectors of the shield where the surrounding soil is compressed, and others where it is relaxed, similar to the TBM behaviour proposed in Broere et al. (2007). Comparing the relative position of the

shield-skin with the excavated profile proves useful in order to demonstrate this behaviour. Fig. 18 reports some results. The colour lines represent the interaction diagram as in Fig. 16b. Each line represents the amount of compression or relaxation of the surrounding soil along the TBM-shield side at a different advance stage. The right end of each coloured line corresponds with the TBM face, the left end (coinciding with the black line) corresponds with the tail. The interaction profiles at intermediate advance steps are in grey. A black line connecting the end points of all the shield-soil interaction lines represents the state of deformation (compression or extension) at the shield tail. Negative values indicate that the TBM has moved towards and into the soil further than the cavity excavated by the cutter head (compressing the soil present) and positive values indicate a gap between shield and soil and possible soil relaxation.

Defining the shield-soil interface displacements as the distance between the shield side and the "virgin" excavated profile makes only sense assuming elastic behaviour for the surrounding soil. On the other hand, an elastic soil model generally provides a poor description of the ground behaviour and response (Muir Wood, 1990). Therefore for proper interpretation of the shield-soil kinematical interaction using the relative displacement of the shield, a non-linear soil model incorporating the full unloading-reloading behavior has to be considered.

At certain advance stages the soil is compressed and then relaxed as the shield advances further. A more realistic quantification of the soil relaxation is then based on the distance between the shield side and the most outward location previously reached in that sector of the excavated profile. The most outward location can either have been caused by the original excavation or by subsequent outward displacement by the shield. In the numerical model (Festa et al. 2015) the excavated cavity undergoes an update for the shield outward displacements. This unloading-reloading behaviour as pictured in Fig. 16 commonly occurs as a result of theoretical tunnel driving, see e.g. Nagel et al. (2010), but also as the result of the true snake-like motion of the shield a discussed by Sugimoto and Sramoon (2002) and shown in Figs. 17 and 18 for this project. A clear example of unloading-reloading is visible in the interval -1580 ÷ -1575 of Fig. 18. In that sector the tail interaction line falls within the grey shadowed area. As this happens in the negative field of the graph, the amount of compression is lower than that already reached at an earlier stage at the same location. Thus, the surrounding soil is unloaded.

4 Soil displacements and TBM's kinematics

The shield-soil interface displacements, as obtained from the kinematical model, and the observed soil response were compared in Figs. 19 through 22. Each graph shows the observed shield-soil interface displacements that occurred at the shield tail, along with the corresponding observed soil response. The horizontal displacements presented are those that occurred at the depth of the tunnel axis. The vertical movements on top of the shield are those measured by the first and second extensometers above the tunnel axis. On the x-axis of the graphs are the (calculated) shield-soil interaction displacement and the (monitored) soil displacements. On the y-axis, is the distance of the shield face from the monitoring section. For example, 0 on the y-axis corresponds to the shield face exactly at the monitoring section, whereas 10 corresponds to the face 10 m after the same instrumented section.

The sign convention partially differs from that adopted in Fig. 18. The convention here matches the intuitive meaning of the side displacements in relation to the position of the tunnel axis. If the shield had no tapering and would perfectly follow the excavated alignment, the tail interaction lines would be vertical lines crossing 0. According to this convention, positive shield-soil interaction represents soil extension on the left-hand side and soil compression on the right-hand one. Vice versa, negative values of shield-soil interaction represent soil compression at the left-hand side and soil extension at the right-hand one.

The shield-soil interaction lines (i.e. interaction displacements) represent the amount of displacement induced at the shield-soil interface by the shield tail. These values have been calculated from a comparison of the position and orientation of the cutter wheel and a stepwise integration of the position and orientation of the TBM shield along the entire tunnel alignment, see Festa et a. 2015 and Section 3 of the present paper for details. As such the interaction displacements represent an independent measurement of the induced displacements at the shield-soil interface and they are compared here with direct (extensometer and inclinometer) measurements of soil deformations at some distance from the shield. In the graphs, when the TBM face is at the monitoring section (0 on the y-axis), the shield tail is 10.235 m behind. Notwithstanding the interaction value is drawn at distance 0,

and not at -10.235.This is to preserve the consistency between the shield-soil interaction and the soil response lines and the values that they represent in time.

First cross-section

At the first cross-section (Fig. 19) horizontally the soil responded differently between first and second crossing. The sector of major interest is between 0 and 10.235 m, between the crossing of the monitoring section by the shield face and its tail, respectively. In said sector, during the first passage, at the shield-soil interface a soil relaxation of between 20 and 40 mm was calculated from the TBM orientation at the left-hand side and a relaxation of 0 to 20 mm at the right-hand one. That was paired with a monitored soil displacement of less than 10 mm from inclinometers at the left-hand side and with a more or less neutral response at the right-hand one. During the second passage at the left hand side a shield-soil interface “gap” of 20 to 60 mm was derived from the TBM data, whereas at the right-hand one the interface displacements ranged between a relaxation of 20 mm and a compression of similar magnitude. The soil responded neutrally as observed from the inclinometer data at the left-hand side, and first converged than expanded at the right-hand one. At the compressed side, this example shows some but limited correlation between the compression at the shield-soil interface and the behaviour of the surrounding soil (second passage – right-hand side).

It is not surprising that the measured displacements are attenuated with respect to those calculated for the shield-soil interface. First of all, the closest borehole where the actual soil movements are recorded was located at 2.50 m from the shield side. Moreover, a plastic zone in the vicinity of the contact area is likely to have occurred, further limiting the spreading at distance of the induced displacements. This latest aspect is also observed in cavity-expansion methods in elastic-plastic soil conditions (Festa et al., 2011). At the relaxed side, even in presence of theoretical extension at the shield-soil interface (left-hand side, both crossings), only a feeble convergence showed during the first crossing and a neutral response during the second. This suggests that a unique deterministic relationship between shield-soil interface displacements and soil response does not exist. Other aspects must have played a role of at least the same order of magnitude as the kinematical interface behaviour.

A further clue may be found in the different vertical response of the soil directly above the tunnel between first and second passage. In the calculated shield-soil interface displacements at the shield tail in the sector of interest (shield face between 0 and 10.235 m) no particular “gaps” or compressions were present. During the first crossing a maximum compression of 10 mm was calculated, opposed to a maximum relaxation of 20 mm during the second crossing. Nevertheless, while during the first passage the measured vertical settlements progressed downward without any measurable rebound, during the second passage a remarkable recovery of the prior settlements took place. These aspects are clearly visible both in the graphs of Fig. 19 at the top side, and Figs. 4 and 5. It also appears that the settlement recovery was particularly effective close to the tunnel top, and less and less effective moving further upward. The response of the extensometer sensor just above the tunnel top shows that the upheave started when the tunnel face was between 5 and 10 m after the control section. This suggests that the tail-void grouting may produce a compensating effect even before the passage of the shield tail across the control section.

Second cross-section

At the second cross-section (Fig. 20), the horizontal soil response was similar but attenuated when compared with that at the first one (Fig. 19). This holds for both crossings. The shield-soil interface displacements were comparable, with “gaps” of 20 to 60 mm calculated at the left-hand side and compressions up to 20 mm at the right-hand one. During the first crossing the surrounding soil actually responded with a slight converging trend at the left hand side and a neutral one at the right-hand one. During the second passing, the convergence at the left-hand side was compensated, and a small expansion at the right-hand side was observed. As for the case of the first cross-section, a unique deterministic relationship does not seem to exist between shield-soil kinematic interface displacements and the soil response. This condition confirms that other aspects must play a role too.

Some differences between the first and second cross-section emerged from the vertical response. During both first and second shield passage the induced settlements were more limited at the second cross-section than at the first one. First of all, at the second cross-section a recovery of the prior settlements was found already during the first passage. That was observed close to the tunnel top (sensor number 3 in BH5, Fig. 20) and is progressively less apparent moving closer to the surface and away from the TBM. The prior settlements were recovered also during the second passage. In this

case two distinct recoveries occurred, the first upon arrival of the shield face at the cross-section, and the second between +5 and +10.235 m, i.e. during the transit of the second half of the shield body. These vertical soil responses were matched with the shield-soil kinematical interaction. During the first crossing the interface interaction at the second cross-section was not dissimilar to that at the first cross-section. During the second crossing, at the first cross-section the shield tail interacted neutrally with the excavated soil, with a relaxation of about 20 mm at about +10 m (near the passage of the shield tail through the monitoring section). In contrast, during the second crossing at the second cross-section the shield tail interacted with the excavated soil resulting in a fluctuation between a relaxation of 20 mm and a compression of the same magnitude. This might have contributed to the reduction of the induced settlements at the second passage of the second section (Fig. 20), compared to second passage in the first section (Fig. 19).

Third cross-section

The difference in terms of soil response between second (Fig. 20) and third (Fig. 21) cross-sections was not deemed relevant. A slightly larger horizontal expansive behaviour (divergence) was observed during the first passage at section 3 (Fig. 21) when compared to the first passage through sections 1 and 2 (Figs. 19 and 20, respectively). Shield-soil interface displacements were similar as well. Also, during the second crossing no relevant differences were observed. When the shield pushes against the surrounding soil – as for example at the right-hand side of the second crossing – a somewhat larger divergence is registered. As already said, the observed displacements were smaller than the ones calculated at the shield-soil interface. This was probably due both to the distance of the borehole from the shield side (1.80 m in this case) and to the plastic deformation of the region of soil closest to the contact area. On the other hand at the left-hand side, where a significant shield-soil interface gap was calculated, limited or no convergence was measured at all. This demonstrates that, assuming the TBM kinematic model is correct, some other relevant process occurred that has not been quantified yet. A likely candidate is the infiltration of tail grout in the region between the shield skin and the excavated soil profile. The partial or complete “compensation” of the converging effect in the sectors where the soil is relaxed was observed at all three cross-sections so far investigated.

The vertical soil response and kinematical interaction at cross-section 3 (Fig. 21) were in line with those at cross-sections 1 and 2. A modest recovery of the prior settlements appeared during the first passage and more markedly during the second one. The graph of the vertical displacements at the top side during the second passage confirmed that settlement recovery is usually achievable close to the tunnel top but much less at distance. This also is a recurrent behaviour observed in all three cross-sections so far investigated.

Fourth cross-section

At the fourth cross-section the horizontal soil response during the first crossing was similar to those already observed at the other sections (Fig. 22). The overall horizontal displacements were almost neutral on both sides. Also the shield-soil horizontal interface displacements during the first crossing were in the range observed at other locations. In contrast, during the second crossing, the horizontal diverging trend was quite symmetrical and larger than at all other sections. The soil relaxation at the shield-soil interface calculated at the left-hand side, with a peak values of 80 mm, was also the largest among all the monitored cross-sections.

The fourth cross-section showed peculiarities also concerning the vertical soil response and the associated shield-soil interface displacements. During the first crossing the shield-tail stayed constantly in contact with the excavated soil, with the calculated interface compression ranging from 0 to 20 mm. That is reflected in one of the smallest settlements so far observed. Moreover, the soil above the tunnel was well supported all along the transit of the shield, and that prevented larger settlements to occur. Those settlements, as seen before, are hardly recoverable once occurred except for the near vicinity of the tunnel being built. During the second crossing of cross-section 4 (Fig. 22) something already seen during the second crossing of cross-section 2 (Fig. 20) occurred. The pronounced recovery of the prior settlements led to an inversion in the direction of the total vertical displacements in the soil sector above the tunnel axis. The vertical displacements turned upward closer to the tunnel, meanwhile farther from the tunnel they remained downward oriented.

Impact of tail grouting

Combining the observations on horizontal and vertical behaviour it seems that even if the shield-soil kinematical interaction plays a role on the tunnelling-induced soil displacements, a similar or even

more important role is played by the grouting process. This is suggested by three observations: 1) often the surrounding soil did not converge towards the tunnel even in presence of a theoretical relaxation at the shield-soil interface; 2) in several circumstances the soil response was more expansive than in others even if the shield-soil kinematical interaction condition was comparable; 3) almost all the recoveries of the prior vertical displacements cannot be explained from kinematics-related reasons. As correctly observed by Standing and Selemetas (2013), innovative approaches are required to correctly predict subsurface displacements. One approach would be to model the complex system of strains induced by the advance of a (slurry-shield) TBM in detail over the entire body of soil surrounding the TBM. Such models would have to account at least for the real kinematic behaviour of the TBM-shield and for the infiltration of the tail void grout between the shield-skin and the surrounding soil when the stress state allows that. However, this falls outside the scope of the current paper. Aspects such as soil excavation at the front, face support, tail-grout consolidation, and loading of the tunnel lining were not part of this research, but have been investigated by Vu et al. (2016). The observed displacement fields point out the limited effectiveness of tail-void grouting in recovering prior settlements. The actual recovery is usually limited to few meters beyond the shield skin. This was already observed in Standing and Selemetas (2013) and is supported by the cavity expansion theory as in Yu (2000). Yu's analytical study of a cylindrical cavity expansion shows that in elastic-perfectly plastic conditions the mass of soil undergoing expansion is limited compared to purely elastic conditions. Yielding occurs in a region surrounding the tunnel, and that region absorbs most of the strains, inducing even more rapid decay of strains further out.

5 Conclusions

TBM tunnel construction in soft soil often induces settlements in the surrounding soil. Most of the current soil-settlement predictions are based on experience gained from previous projects, expressed as a volume loss. However, while volume loss is a good marker of the overall quality of the tunnel construction, it performs rather poorly when used to explain the physical mechanisms that induce those settlements. For instance, aspects such as the TBM features and its real kinematic behaviour when driven through the soil are not yet incorporated in soil-settlement prediction models and cannot be addressed via the volume loss model.

In this paper TBM monitoring data and subsurface soil displacements from a project in The Netherlands were used to compare the TBM-shield kinematic behaviour with the soil response. At each consecutive TBM advance, the actual spatial position of the shield was compared with the excavated soil profile. The comparison enabled the quantification of the displacements induced by the advancing shield calculated at the shield-soil interface, and in particular to distinguish the sectors where the excavated cavity was compressed from those where that was extended. The actual displacements in the surrounding soil were measured using extensometers and inclinometers.

These measurements show that the heave induced by the face support pressure or tail grouting is localized and dissipates quickly with distance. They also show that horizontal soil displacements are not equal on both sides of the TBM. Furthermore, expansive behaviours (compressive strains) tend to dissipate very quickly through the soil at increasing distance from the tunnel, which means that prior settlement recovery is usually achievable close to the tunnel top but much less at distance.

Even more importantly, a unique deterministic relationship between shield-soil interface displacements and soil response does not exist. Other aspects must have played a role of at least the same order of magnitude as the kinematical interface behaviour. The tail-void grouting may play an essential role not only in filling-in the tail void but also in compensating for the kinematical effects of shield advance. Therefore, further research on the correlation between TBM-shield kinematics and induced soil displacements should also be based on accurate measurement of the grouting volumes and pressure in the tail void and, possibly, around the shield skin. A detailed numerical model of the process of grout injection and infiltration within the shield-soil interface will be beneficial.

6 Acknowledgements

The helpful and patient contribution of Vincent Schuurmans (Fugro Ingenieursbureau BV) in supporting the processing of the subsurface monitoring data is kindly acknowledged.

7 References

Bezuijen, A., 2007, *Bentonite and grout flow around a TBM*, ITA-World Tunnel Congress 2007, Underground Space – the 4th Dimension of Metropolises, Prague, 5 May 2007 through 10, pp. 383 – 388 (digital version)

Broere, W., Faassen, T.F., Arends, G., van Tol. A.F., 2007, *Modelling the boring of curves in (very) soft soils during microtunnelling*. Tunneling and Underground Space Technology, 22(5–6):600–609.

Festa, D., Broere, W., Bosch, J.W., 2015, *Kinematic behaviour of a Tunnel Boring Machine in soft soil: theory and observations*, Tunnelling and Underground Space Technology, 49:208–217.

Festa, D., Broere, W., Bosch, J.W., 2013, *Tunnelling in soft soil: Tunnel Boring Machine operation and soil response*, International Symposium on Tunnelling and Underground Space Construction for Sustainable Development, Seoul, Korean Tunnelling and Underground Space Association

Festa, D., Broere, W., Bosch, J.W., 2012, *An investigation into the forces acting on a TBM during driving – Mining the TBM logged data*, Tunnelling and Underground Space Technology, Vol. 32, pp. 143-157

Festa, D., Broere, W., Bosch, J.W., 2011, *Tunnel–boring process in soft soils: improved modelling for reliability enhancement. Kinematic behaviour and tail grouting monitoring*, ITA-World Tunnel Congress 2011, Underground Spaces in the Service of a Sustainable Society, Helsinki, 20 May 2013 through 26, pp. 184-185 + extended digital version

Kasper, T., Meschke, G., 2006, *On the influence of face pressure, grouting pressure and TBM design in soft ground tunnelling*, Tunnelling and Underground Space Technology, 21(2), 160-171

Komiya, K., Soga, K., Akagi, H., Hagiwara, T., and Bolton, M. D., 1999, *Finite element modeling of excavation and advancement processes of a shield tunneling machine*, Soils and Foundations, 39(3), 37-52

Lance, G.A. and Anderson, J.M., 2006, The risk to third parties from bored tunnelling in soft ground, HSE – Health and Safety Executive, Research Report 453, Norwich

Mair, R.J., Taylor, R.N., 1993, *Prediction of clay behaviour around tunnels using plasticity solutions*, Predictive Soil Mechanics. Proceedings of the Worth Memorial Symposium, 27-29 July 1992, St. Catherine's College, Oxford, pp. 449-463

Mair, R.J. and Taylor R.N., 1997, Bored tunnelling in the urban environment. State-of-the-art Report and Theme Lecture, Proceedings of 14th International Conference on Soil Mechanics and Foundation Engineering, Hamburg, Balkema, Vol. 4., 2353-2385

Mair, R.J., Taylor, R.N., & Bracegirdle,A., 1993, *Subsurface settlement profiles above tunnels in clay*, Géotechnique 43, No. 2, pp. 315-320

Mair, R.J., Taylor, R.N., Burland, J.B., 1996, *Prediction of ground movements and assessment of risk of building damage due to bored tunnelling*, International Symposium on Geotechnical Aspects of Underground Construction in Soft Ground, Balkema, Pages: 713-718

Muir Wood, D., 1990, *Soil behaviour and critical state soil mechanics*, Cambridge University Press

Nagel, F.J., 2009, *Numerical modelling of partially saturated soil and simulation of shield-supported tunnel advance*, Ph.D. Thesis, Ruhr-University Bochum

Nagel, F., Stascheit, J., and Meschke, G., 2010, *Process-oriented numerical simulation of shield tunneling in soft soils*, Geomechanics and Tunnelling, 3(3), 268-282

Peck, R.B., 1969, *Deep excavations and tunnelling in soft ground*. Proc. 7th International Conference Soil Mechanics and Foundation Engineering, Mexico City, State of the Art Volume, 225-290

Standing, J.R., Selemetas, D., 2013, *Greenfield ground response to EPBM tunnelling in London Clay*, Géotechnique 63, No. 12, pp. 989-1007

Sugimoto M. et al., 2007, *Simulation of Shield Tunnelling Behavior along Curved Alignment in a Multilayered Ground*, Journal of Geotechnical and Geoenvironmental Engineering, 133(6), 684-694

Sugimoto, M. and Sramoon, A., 2002, *Theoretical model of shield behavior during excavation. I: Theory*. Journal of Geotechnical and Geoenvironmental Engineering, 128(2), 138–155

Verruijt, A., 1997, *A complex variable solution for a deforming circular tunnel in an elastic halfplane*. International Journal for Numerical and Analytical Methods in Geomechanics, Vol. 21., 77-89

Vu, M.N., Broere, W., Bosch, J.W., 2015, *Effects of cover depth on ground movements induced by shallow tunnelling*. Tunnelling and Underground Space Technology, Vol. 50 pp. 499–506.

Vu, M.N., Broere, W., Bosch, J.W., 2016, *Volume loss in shallow tunnelling*. Tunnelling and Underground Space Technology (Revision submitted 2016).

Yu, Hai-Sui, 2000, *Cavity Expansion Methods in Geomechanics*, Springer Science + Business Media Dordrecht

Table Captions

Table 1. Range of soil parameters for the Hubertus tunnel project

Layer #	Description	q_c [Mpa]	γ_{dry} [kN/m^3]	γ_{sat} [kN/m^3]	c' [kPa]	φ' [°]
1	Anthropogenic soil	0.1 2.0	16.8 19.2	17.8 20.2	0	25 31.4
2	Manmade sand dune	4.1 13.6	14.0 16.8	18.7 20.2	0	26.9 39.6
3	Moderately compact recent beach sand	3.5 13.7	14.7 16.2	19.0 19.9	0	32.6 36.2
4	Silt lens	1.0 8.2	13.0 14.4	18.0 18.9	0	25.0 31.4
5	Peat (Hollandveen)	1.1 3.2	1.7 6.9	9.5 13.3	10 15	15.0 18.8
6	Sand lens	2.9 7.4	12.8 14.6	17.3 19.6	0	30.0 37.7
7	Moderately compact dune sand	6.9 15.6	13.9 15.8	17.8 20.1	0	31.0 38.9
8	Highly compact beach sand	17.3 38.7	14.9 15.7	19.2 19.6	0	35.6 43.4
9	Sand with local silty and clayey layers	2.4 15.3	12.6 15.8	17.7 19.7	0	25.3 38.2
10	Enclosed sand layers	4.9 21.9	13.9 15.8	17.7 20.3	0	30.0 37.7
11	Sand with thin silty layers	9.4 19.5	14.9 16.1	19.2 19.9	0	27.7 35.8
12	Very compact old beach sand	21.0 40.1	15.1 16.1	19.3 19.9	0	32.6 41.6
13	Clay with silt and sand	3.1 7.8	14.1 16.1	18.1 20.5	0	28.0 35.2
14	Loose to moderately compact sand	11.1 22.9	14.4 15.7	18.9 19.7	0	28.3 36.7
15	Clay lens	1.6 5.1	4.5 5.1	11.4 12.9	10 15	25.0 31.4
16	Loam with some sand	6.1 13.5	11.1 14.0	16.8 18.6	0	27.5 34.5
17	Very compact, medium to coarse river sand	28.2 52.2	15.1 16.1	19.3 19.9	0	38.0 47.7

Table 2. Locations of monitoring sections – south tunnel

	Section 1	Section 2	Section 3	Section 4
Extensometers	Km -1+588.16	Km -1+556.51	Km -1+149.01	Km -1+095.42
Inclinometers	Km -1+586.59	Km -1+555.22	Km -1+147.87	Km -1+094.20

Table 3. Locations of monitoring sections – north tunnel

	Section 1	Section 2	Section 3	Section 4
Extensometers	Km -1+600.57	Km -1+571.24	Km -1+161.58	Km -1+108.04
Inclinometers	Km -1+599.40	Km -1+570.15	Km -1+160.32	Km -1+106.73

Figure Captions

Figure 1. Longitudinal cross-section of the TBM used at Hubertus tunnel

Figure 2. Plan view and stratigraphy of the south tube

Figure 3. Explanation of symbols for extensometers

Figure 4. Extensometers and settlement troughs at monitoring section 1 – first passage (left tube) – south tunnel – 2006

Figure 5. Extensometers and settlement troughs at monitoring section 1 – second passage (right tube) – north tunnel – 2007

Figure 6. Extensometers and settlement troughs at monitoring section 2 – first passage (left tube) – south tunnel – 2006

Figure 7. Extensometers and settlement troughs at monitoring section 2 – second passage (right tube) – north tunnel – 2007

Figure 8. Extensometers and settlement troughs at monitoring section 3 – first passage (left tube) – south tunnel – 2006

Figure 9. Extensometers and settlement troughs at monitoring section 3 – second passage (right tube) – north tunnel – 2007

Figure 10. Extensometers and settlement troughs at monitoring section 4 – first passage (left tube) – south tunnel – 2006

Figure 11. Extensometers and settlement troughs at monitoring section 4 – second passage (right tube) – north tunnel – 2007

Figure 12. Inclinometers at monitoring section 1 – first passage (left tube) and second passage (right tube). The displacements are in mm.

Figure 13. Inclinometers at monitoring section 2 – first passage (left tube) and second passage (right tube). The displacements are in mm.

Figure 14. Inclinometers at monitoring section 3 – first passage (left tube) and second passage (right tube). The displacements are in mm.

Figure 15. Inclinometers at monitoring section 4 – first passage (left tube) and second passage (right tube). The displacements are in mm.

Figure 16. Kinematical shield-soil interaction – Theoretical model

Figure 17. Partial deviations from the planned tunnel alignments – Observed

Figure 18. Example of shield-soil interface displacements around monitoring section #1 – north tube

Figure 19. Shield-soil interaction and soil response – cross-section 1

Figure 20. Shield-soil interaction and soil response – cross-section 2

Figure 21. Shield-soil interaction and soil response – cross-section 3

Figure 22. Shield-soil interaction and soil response – cross-section 4

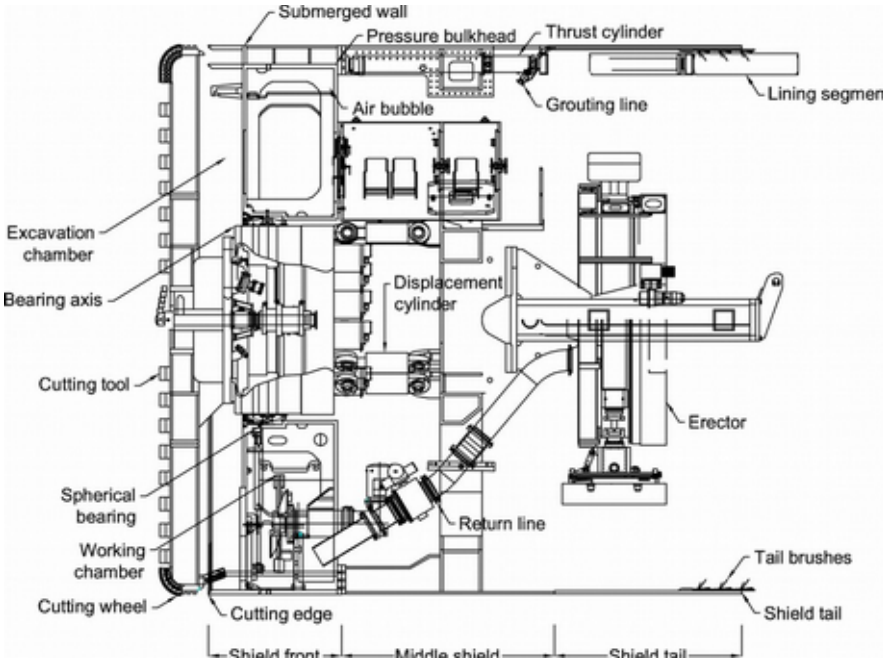

Figure 1. Longitudinal cross-section of the TBM used at Hubertus tunnel

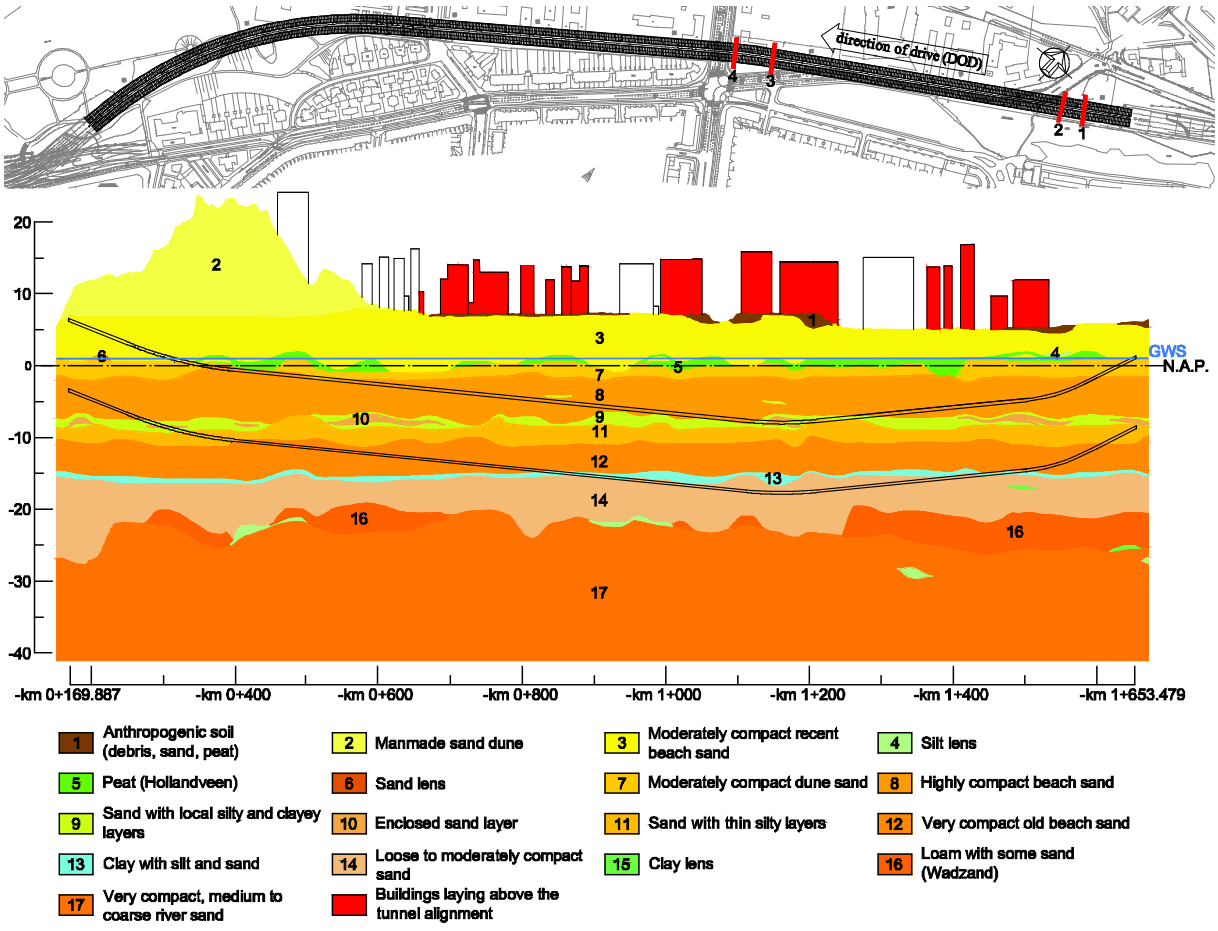

Figure 2. Plan view and stratigraphy of the southern tube

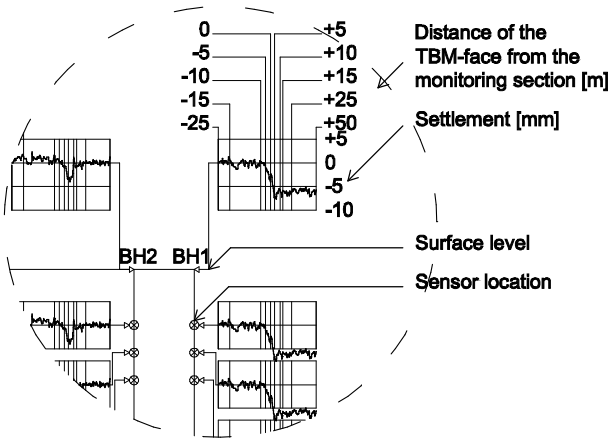

Figure 3. Explanation of symbols for extensometers

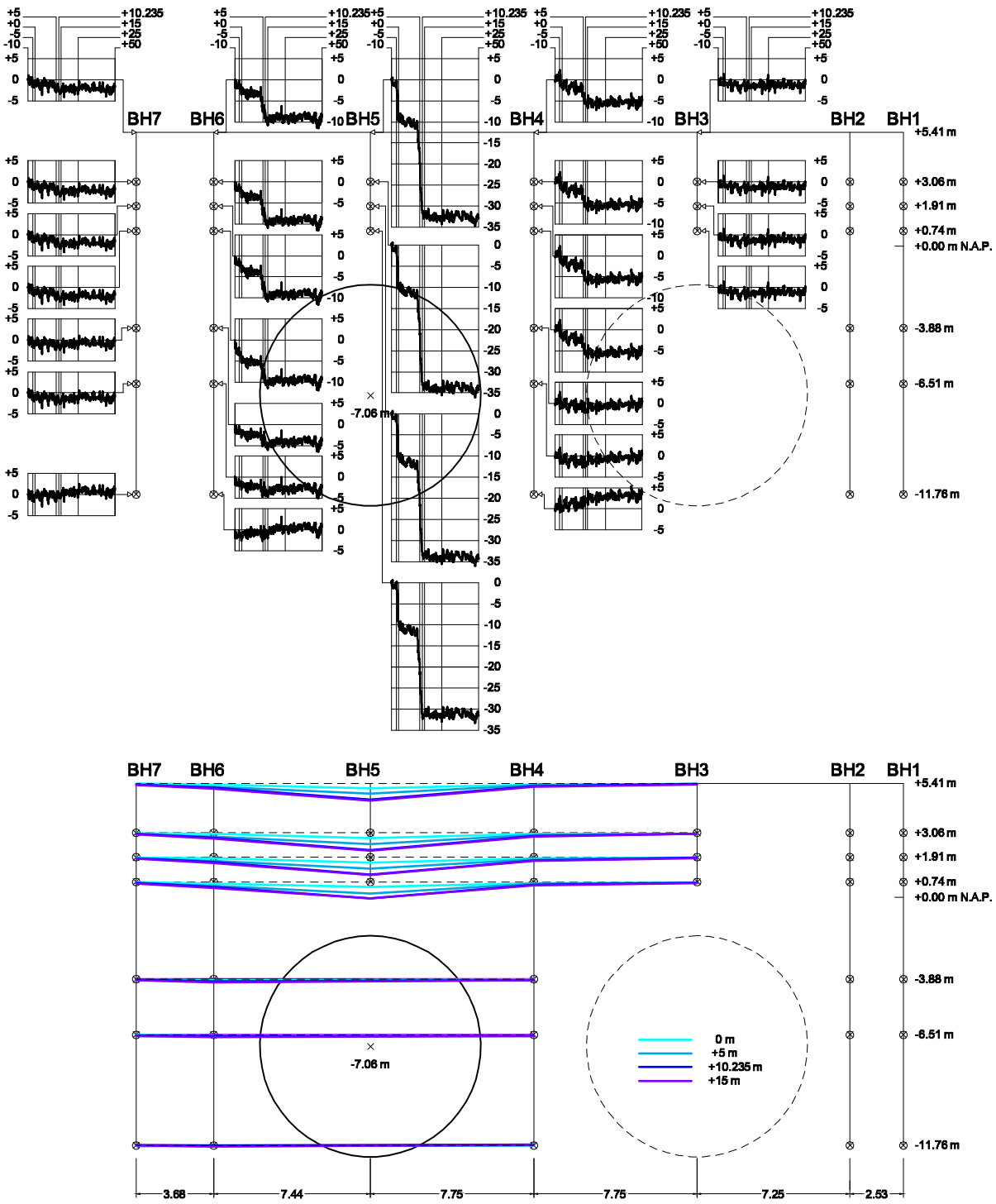

Figure 4. Extensometers and settlement troughs at monitoring section 1 – first passage (left tube) – south tunnel – 2006

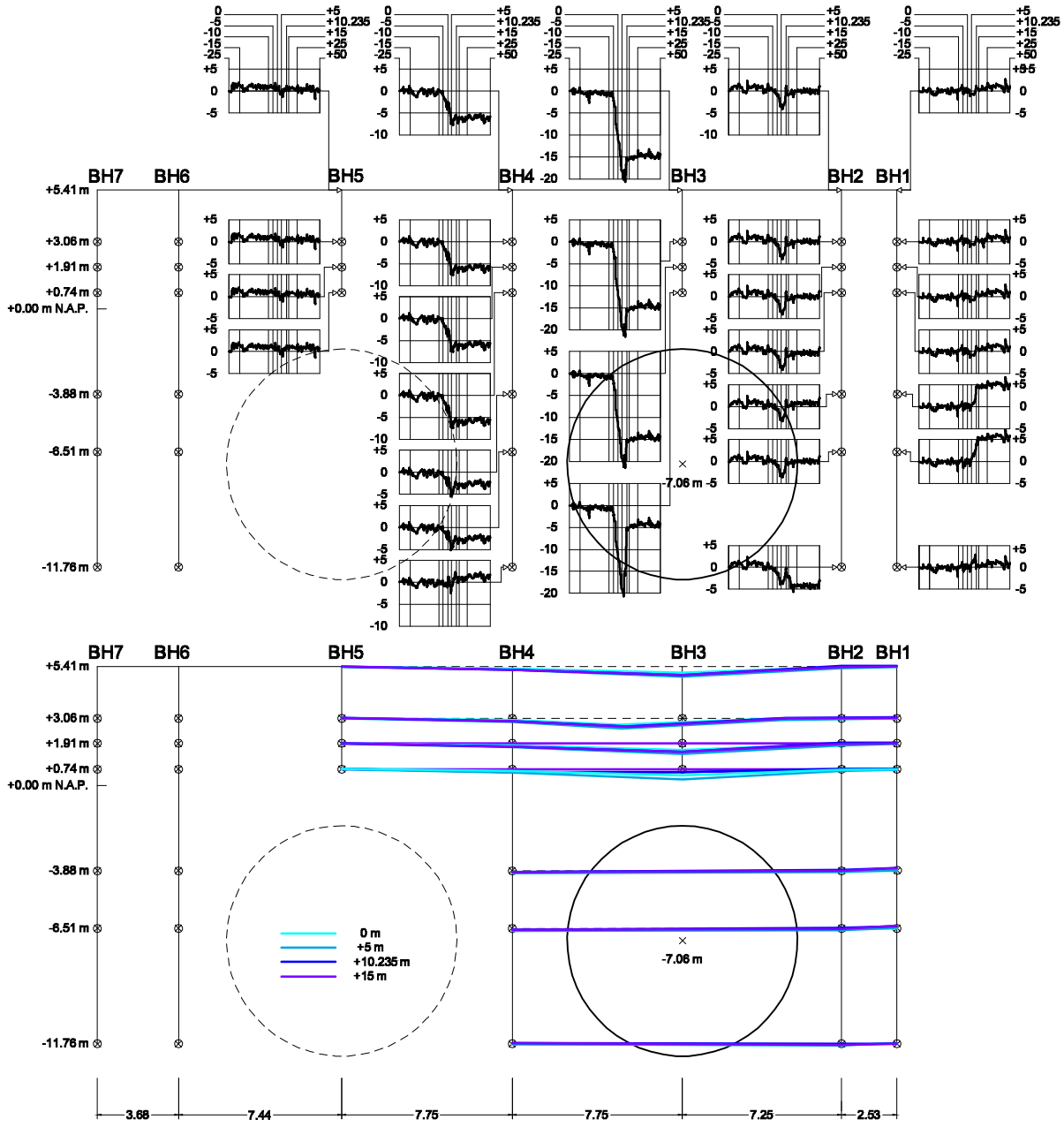

Figure 5. Extensometers and settlement troughs at monitoring section 1 – second passage (right tube) – north tunnel – 2007

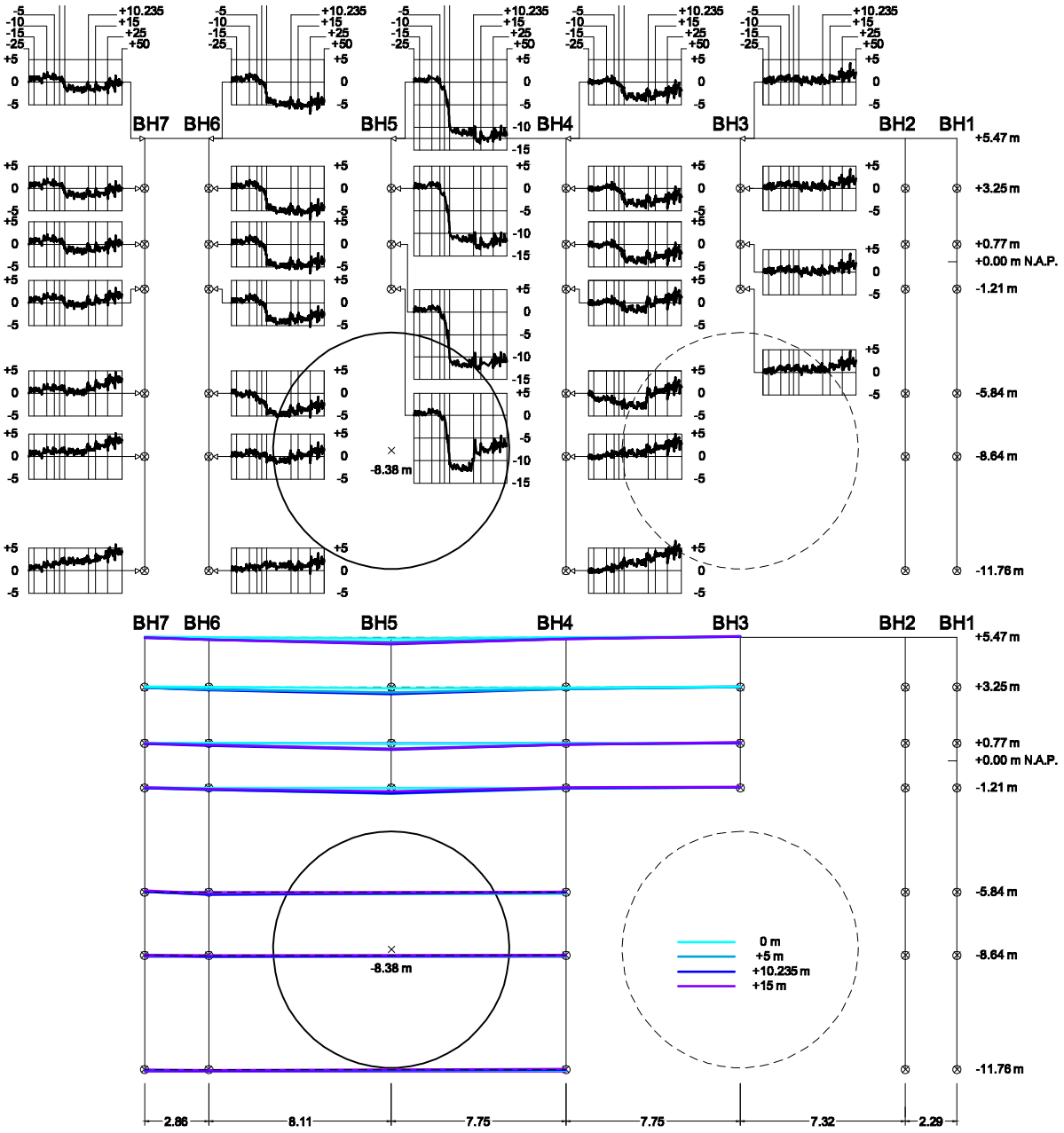

Figure 6. Extensometers and settlement troughs at monitoring section 2 – first passage (left tube) – south tunnel – 2006

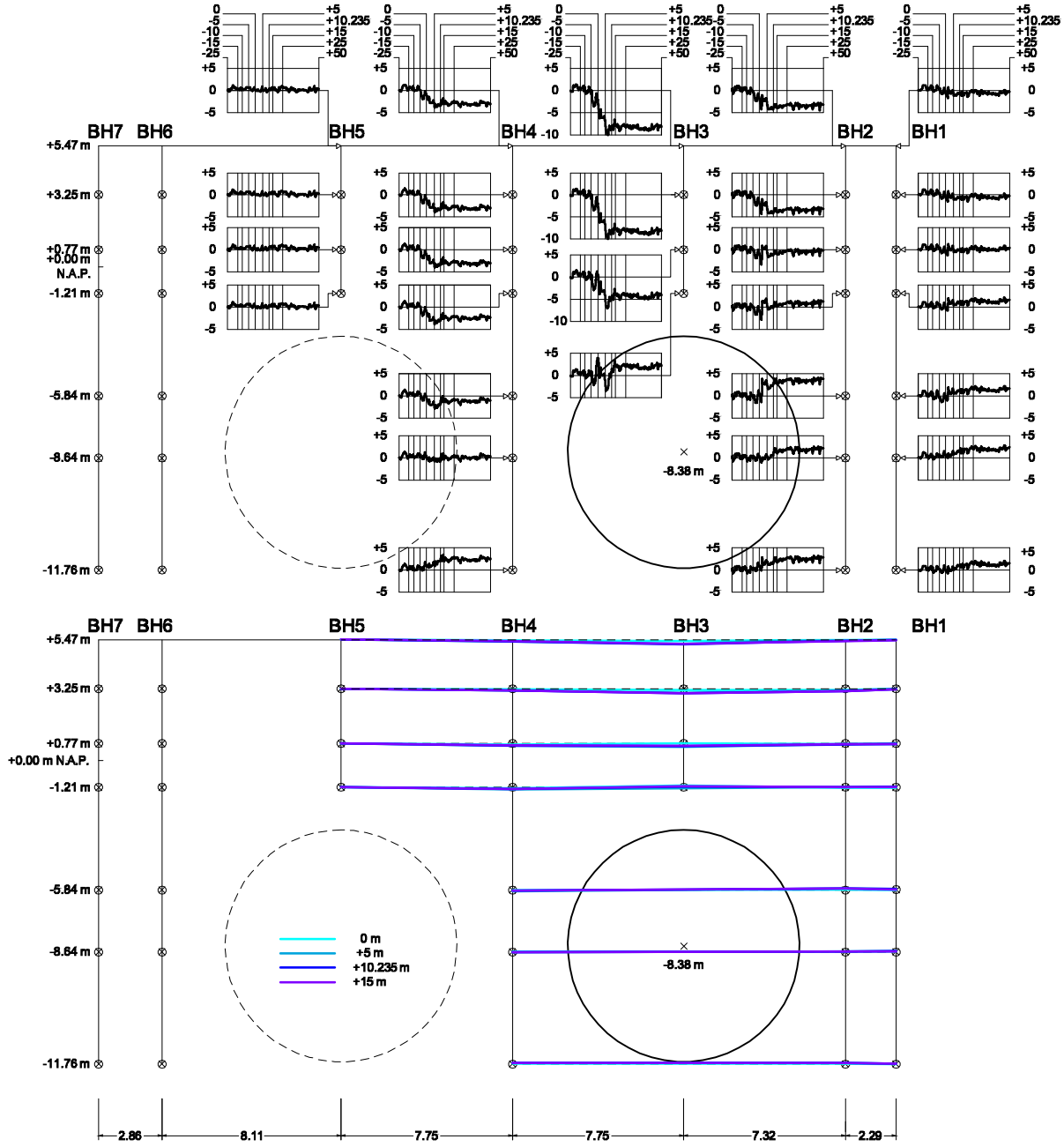

Figure 7. Extensometers and settlement troughs at monitoring section 2 – second passage (right tube) – north tunnel – 2007

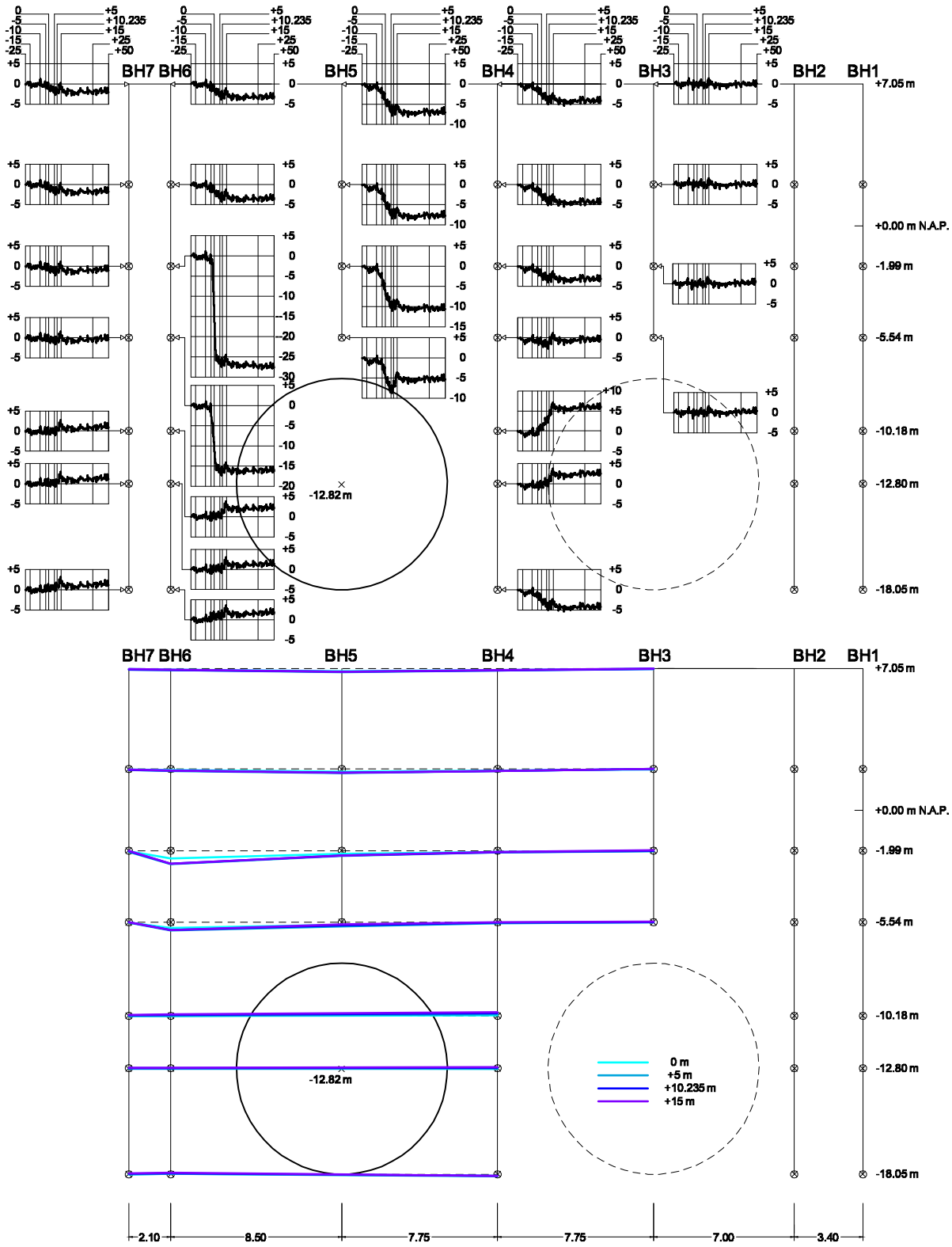

Figure 8. Extensometers and settlement troughs at monitoring section 3 – first passage (left tube) – south tunnel – 2006

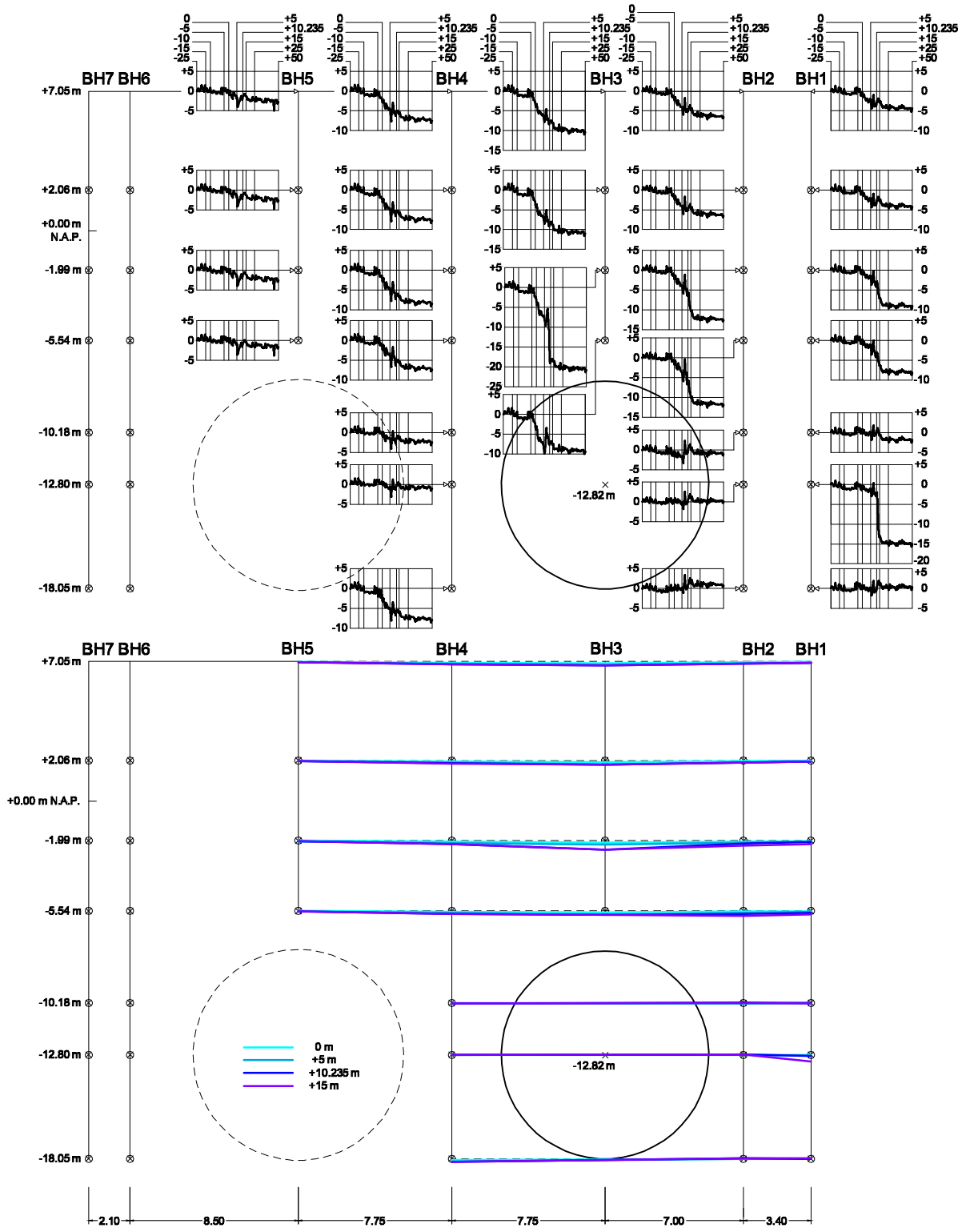

Figure 9. Extensometers and settlement troughs at monitoring section 3 – second passage (right tube) – north tunnel – 2007

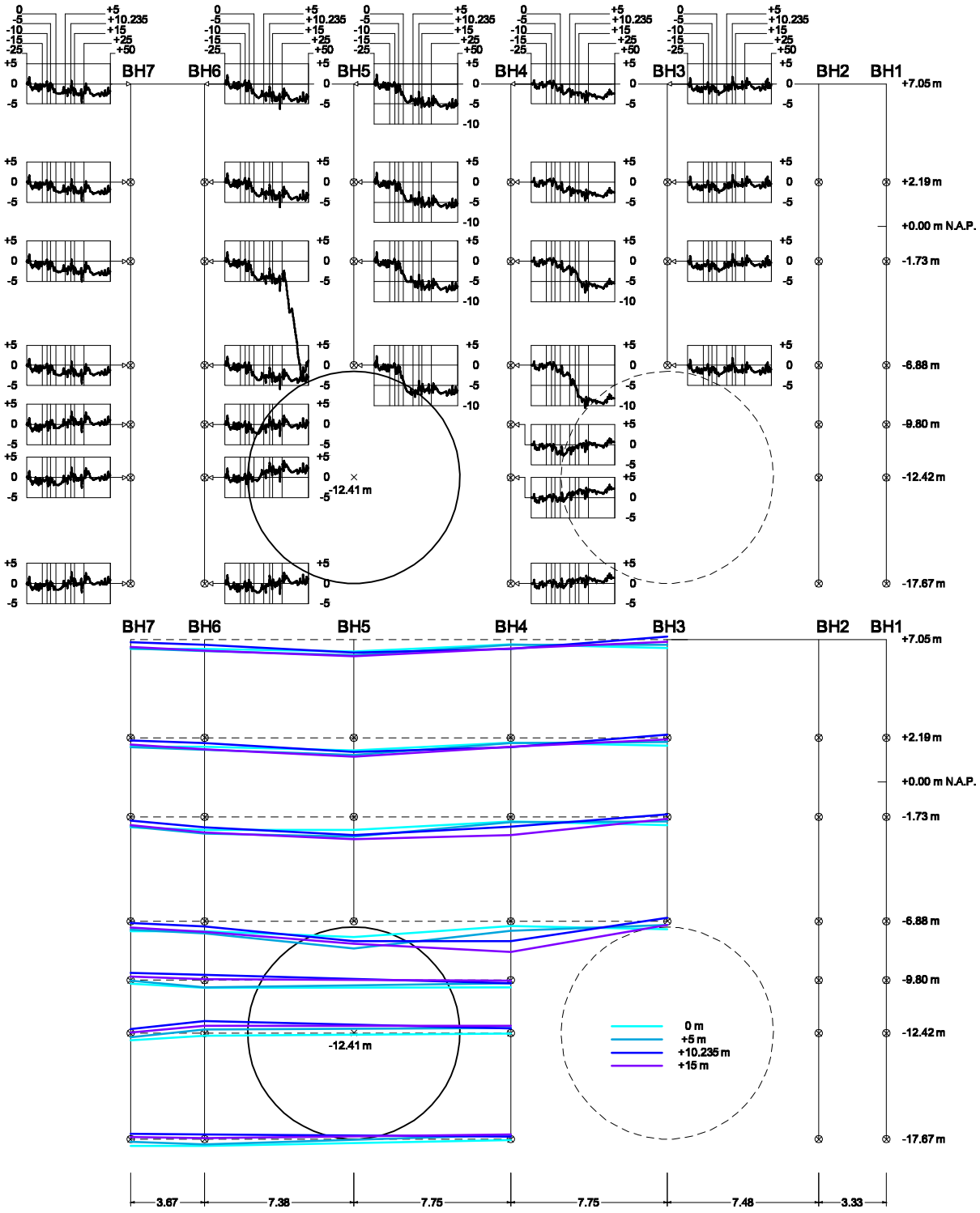

Figure 10. Extensometers and settlement troughs at monitoring section 4 – first passage (left tube) – south tunnel – 2006

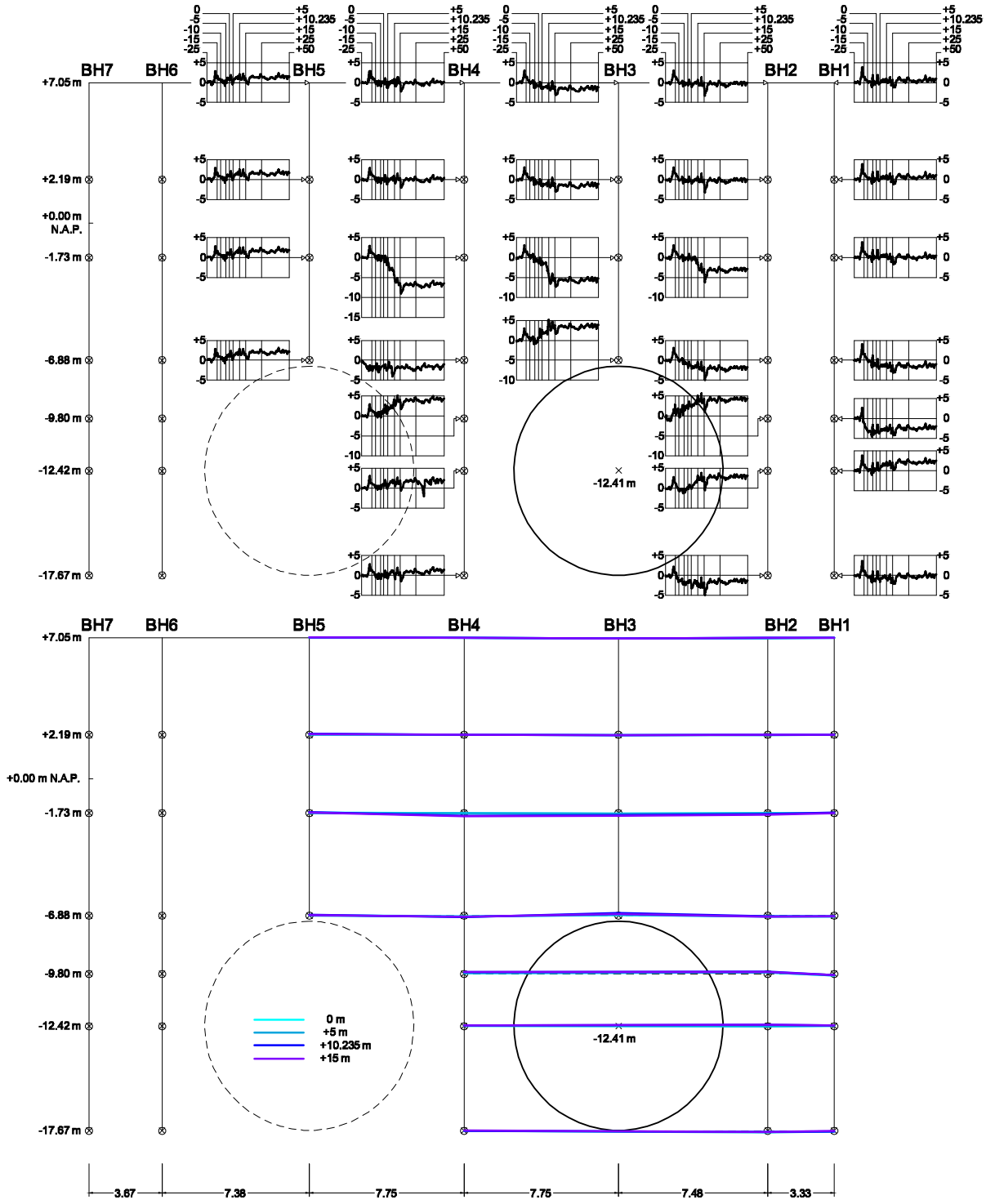

Figure 11. Extensometers and settlement troughs at monitoring section 4 – second passage (right tube) – north tunnel – 2007

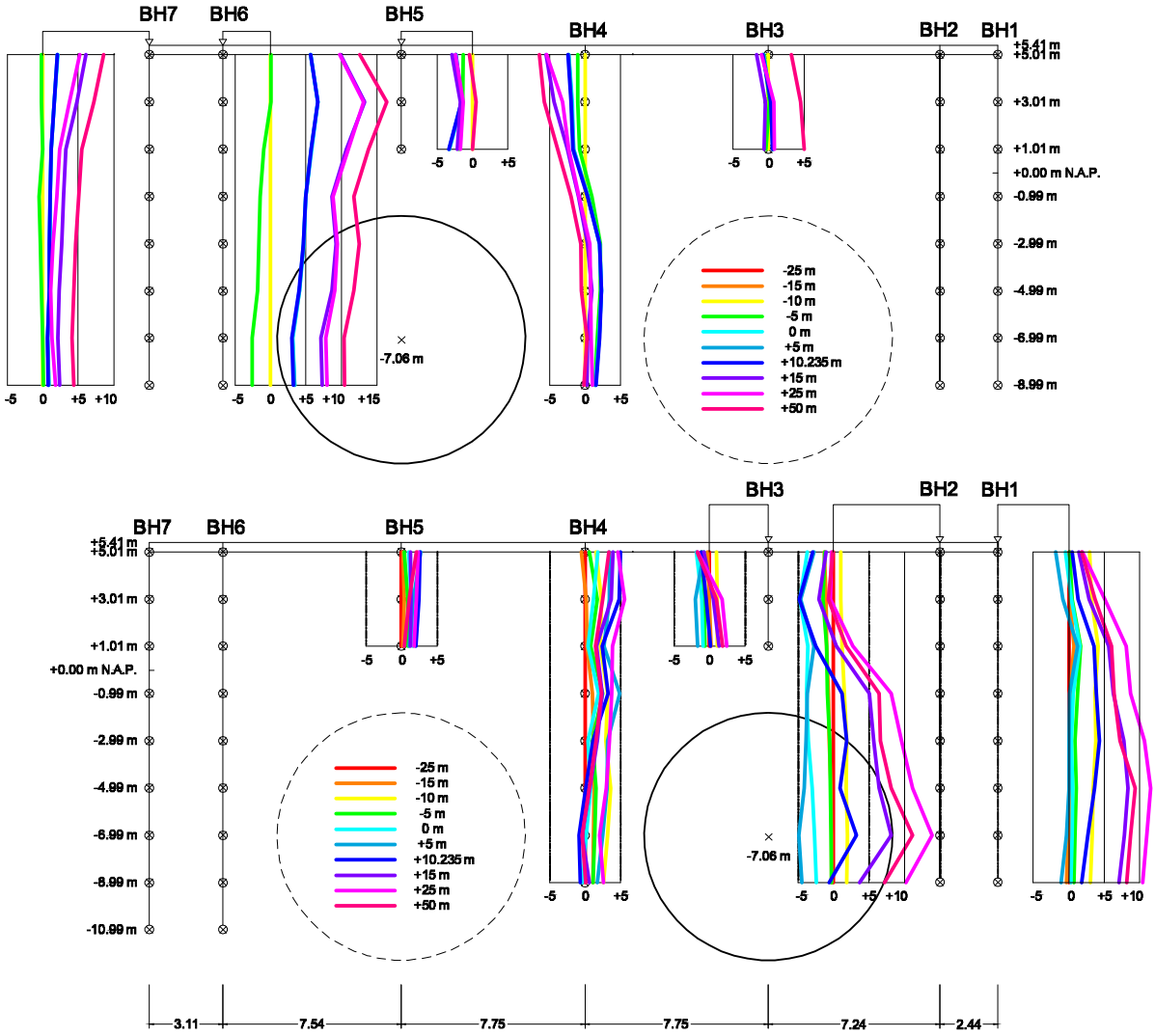

Figure 12. Inclinometers at monitoring section 1 – first passage (left) and second passage (right). The displacements are in mm.

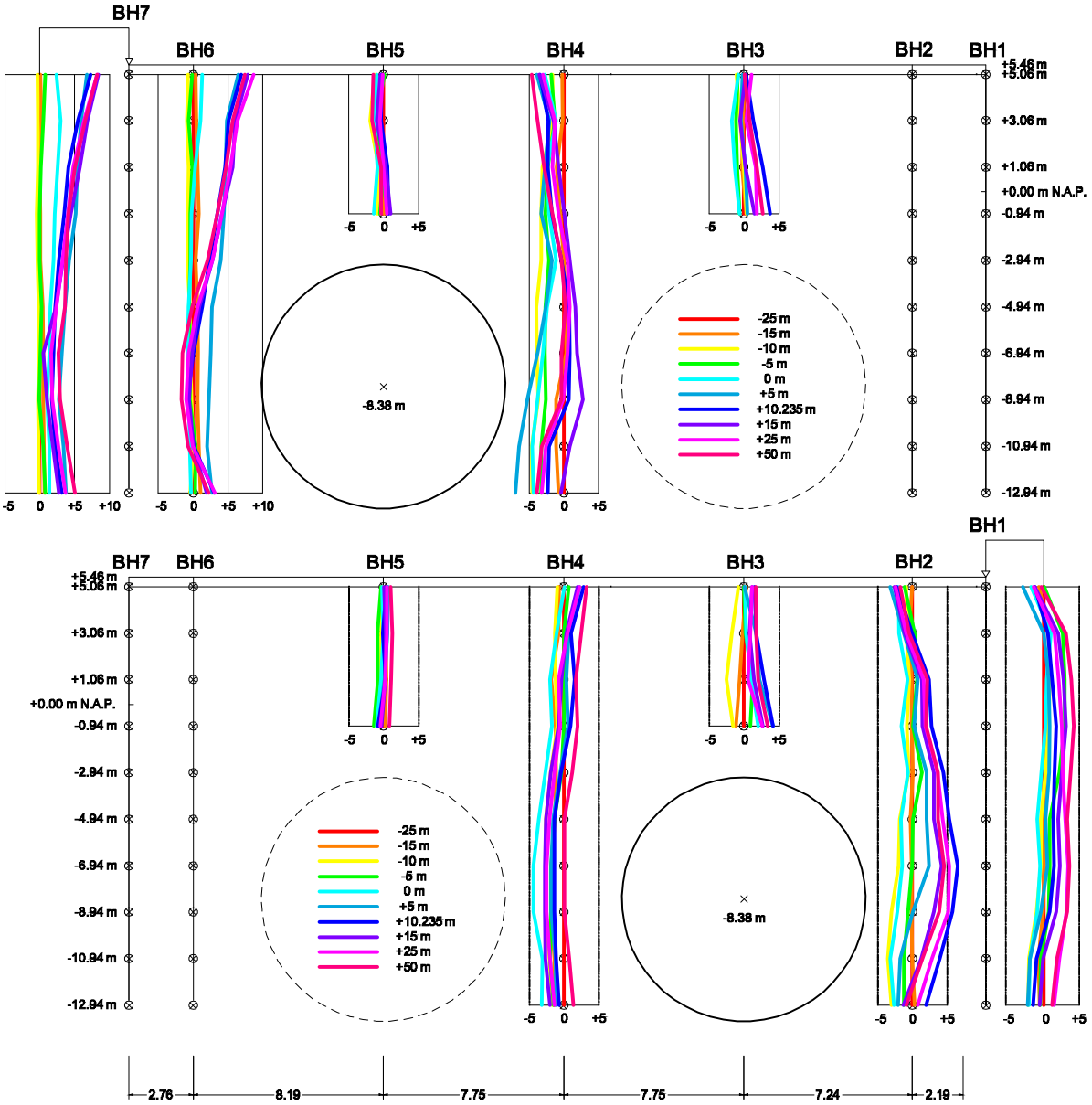

Figure 13. Inclinometers at monitoring section 2 – first passage (left) and second passage (right). The displacements are in mm.

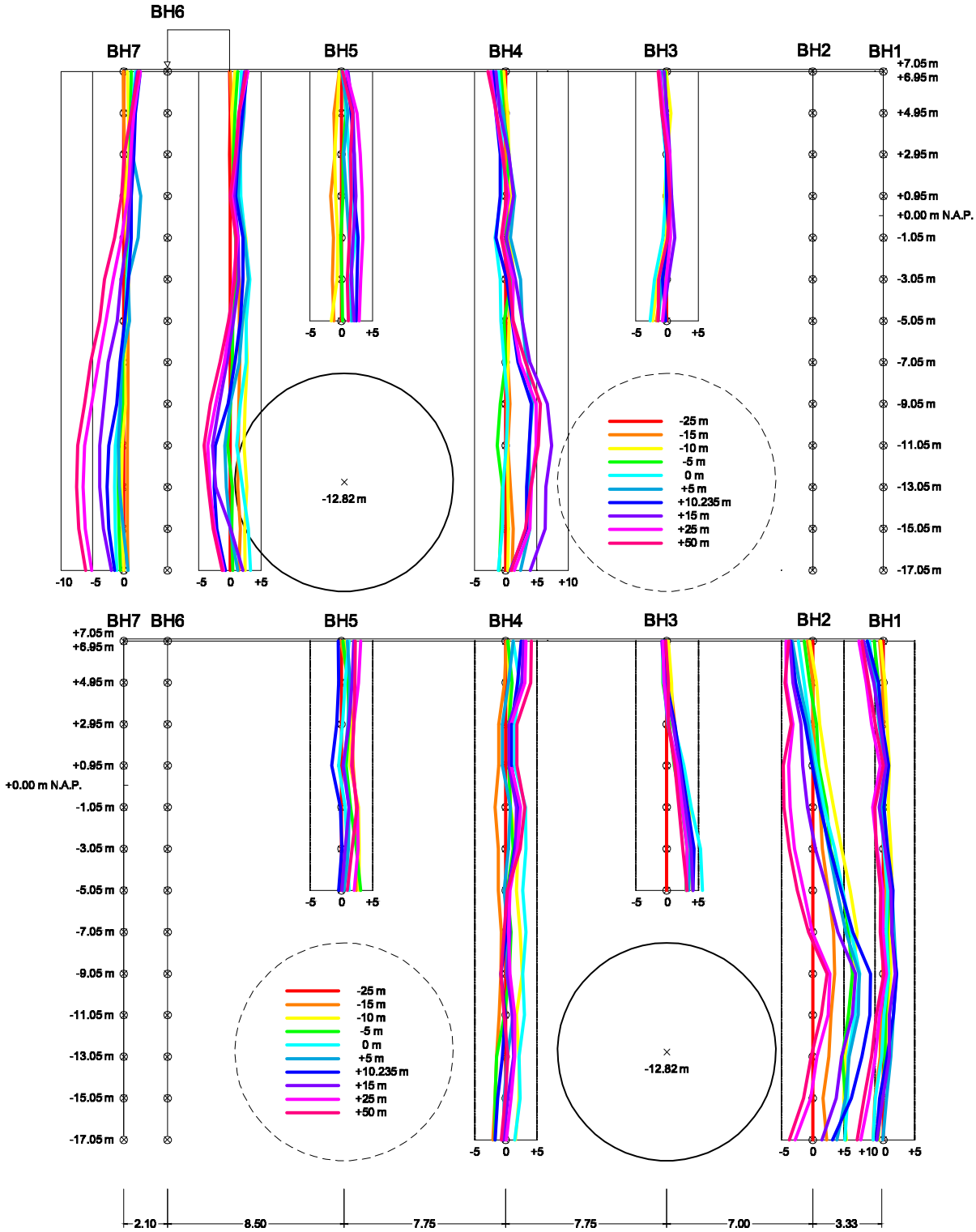

Figure 14. Inclinometers at monitoring section 3 – first passage (left) and second passage (right). The displacements are in mm.

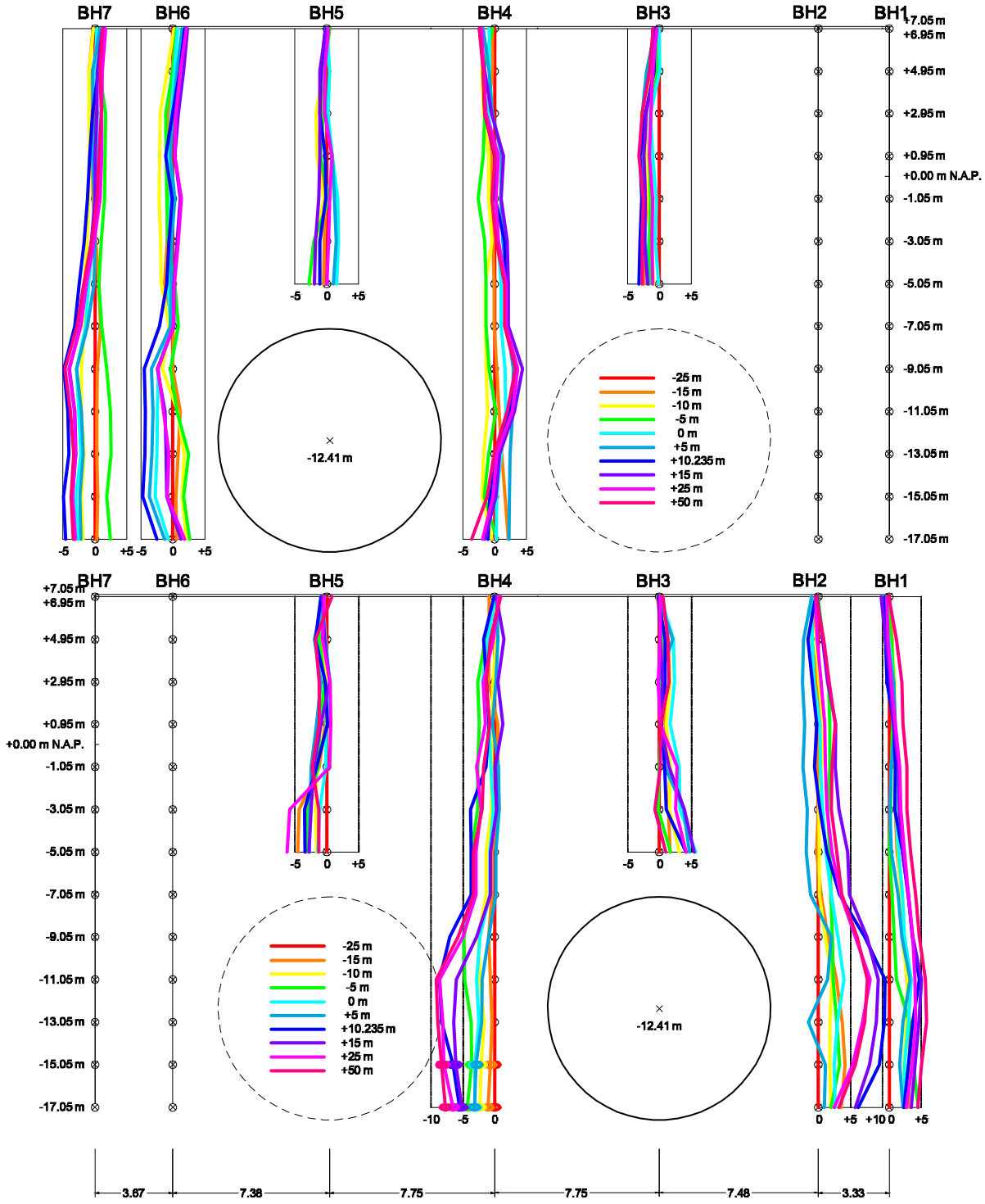

Figure 15. Inclinometers at monitoring section 4 – first passage (left) and second passage (right). The displacements are in mm.

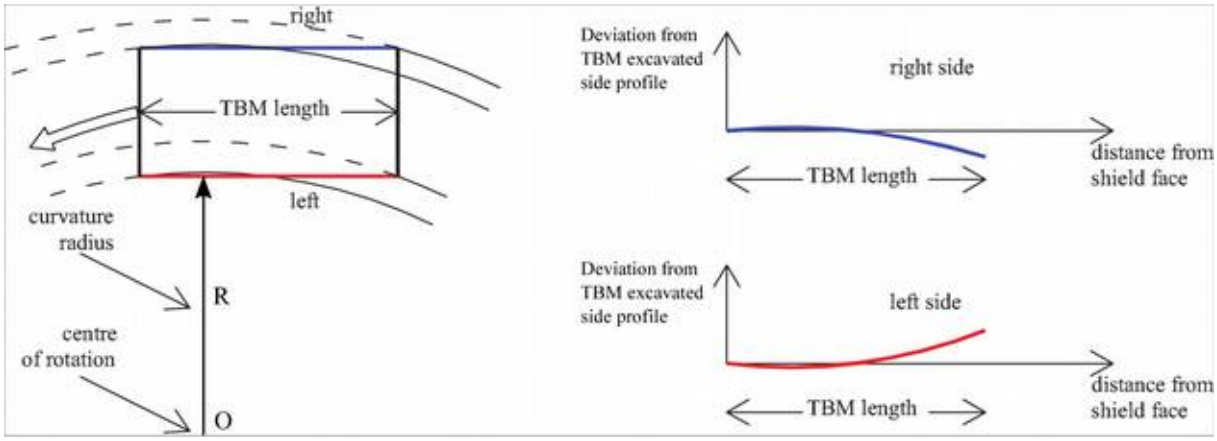

(a) (b)

Figure 16. Kinematical shield-soil interaction – Theoretical model

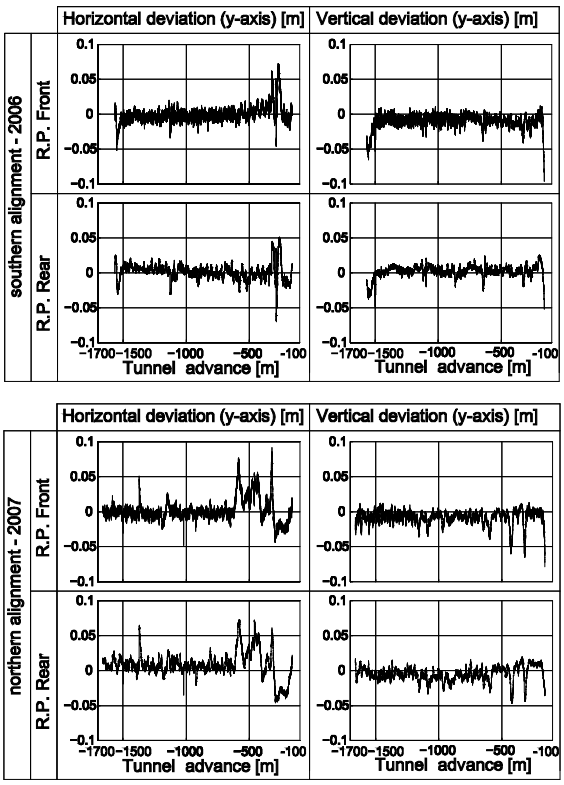

Figure 17. Partial deviations from the planned tunnel alignments - Observed

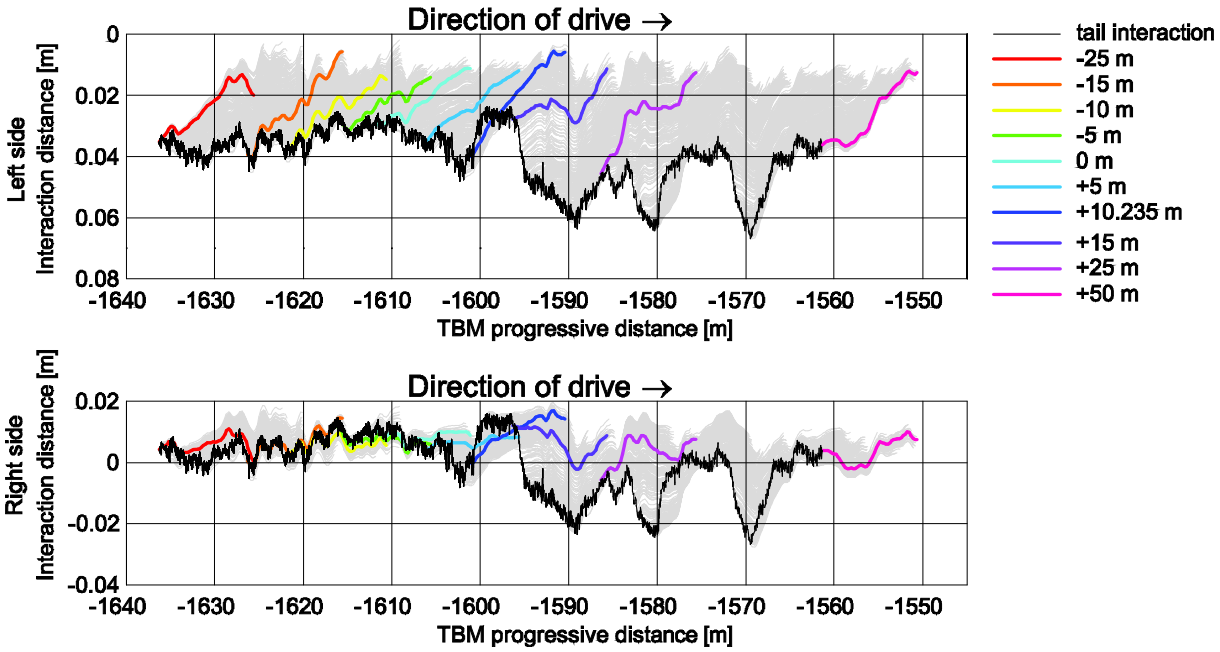

Figure 18. Example of shield-soil interface displacements around monitoring section #1 – north tube

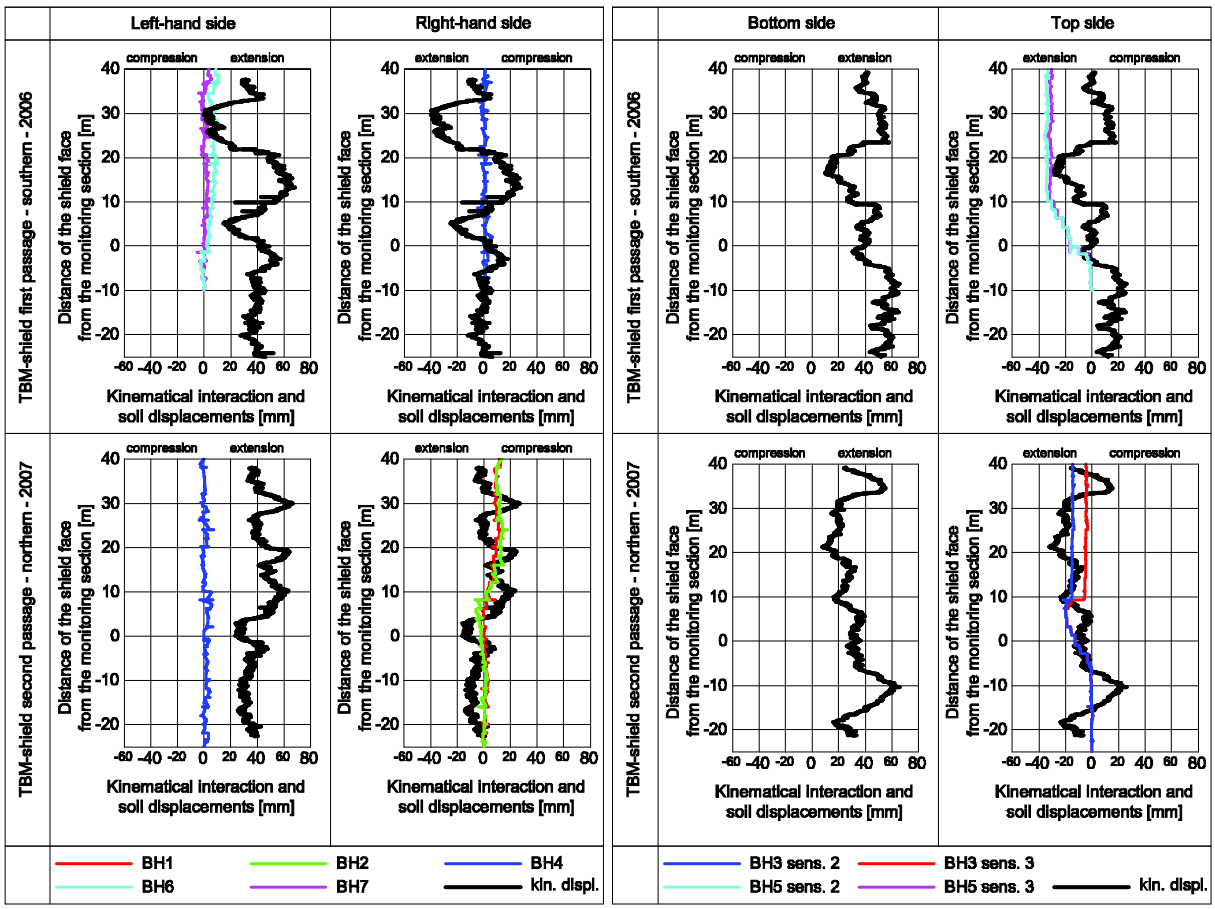

Figure 19. Shield-soil interaction and soil response – cross-section 1

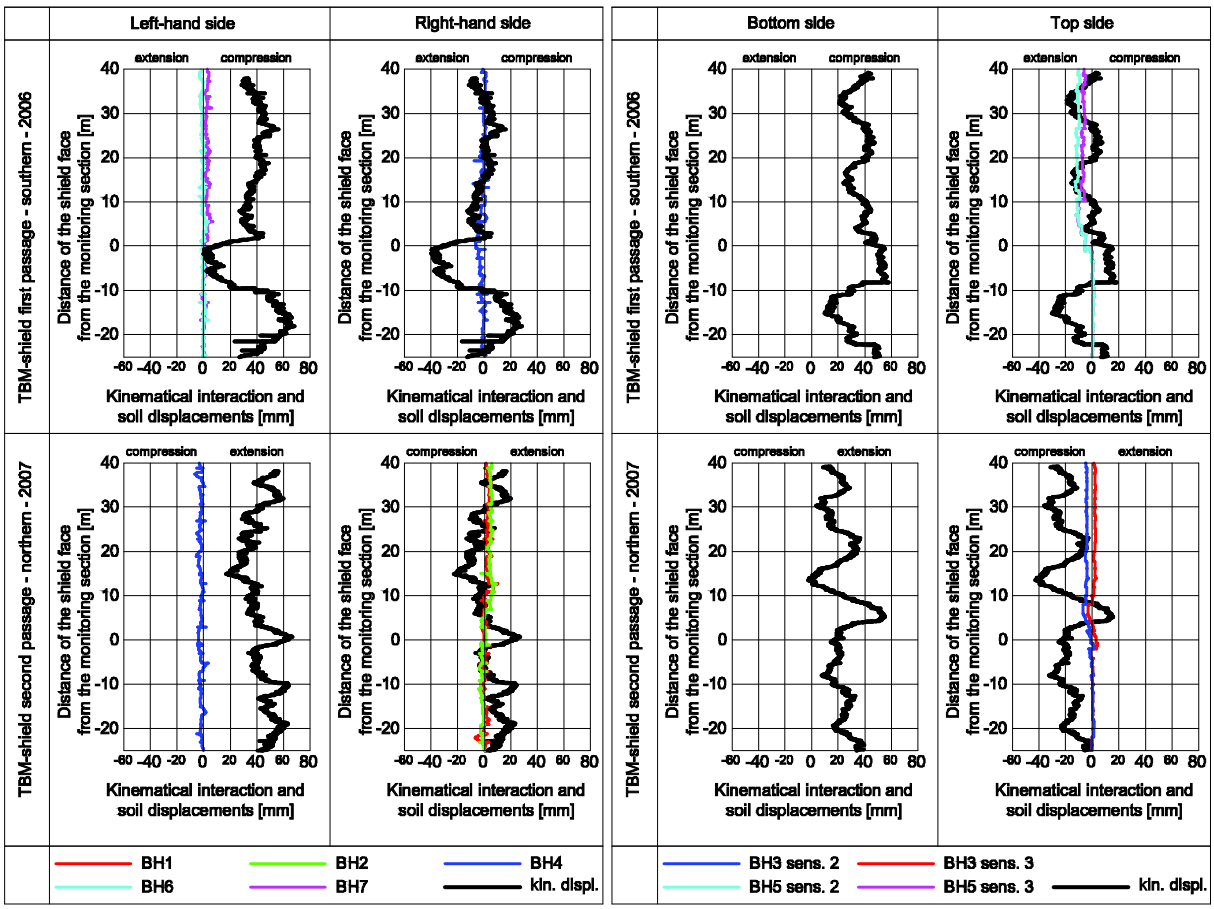

Figure 20. Shield-soil interaction and soil response – cross-section 2

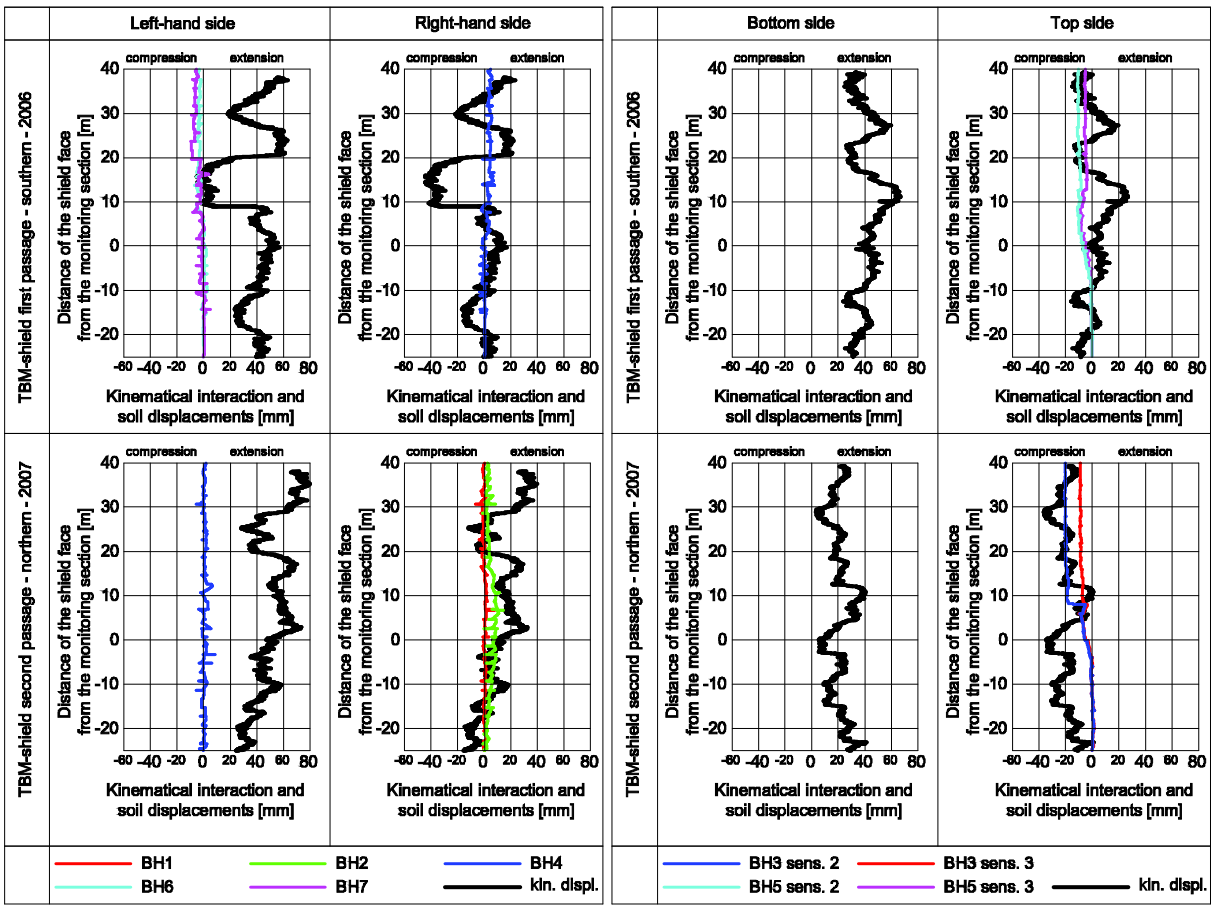

Figure 21. Shield-soil interaction and soil response – cross-section 3

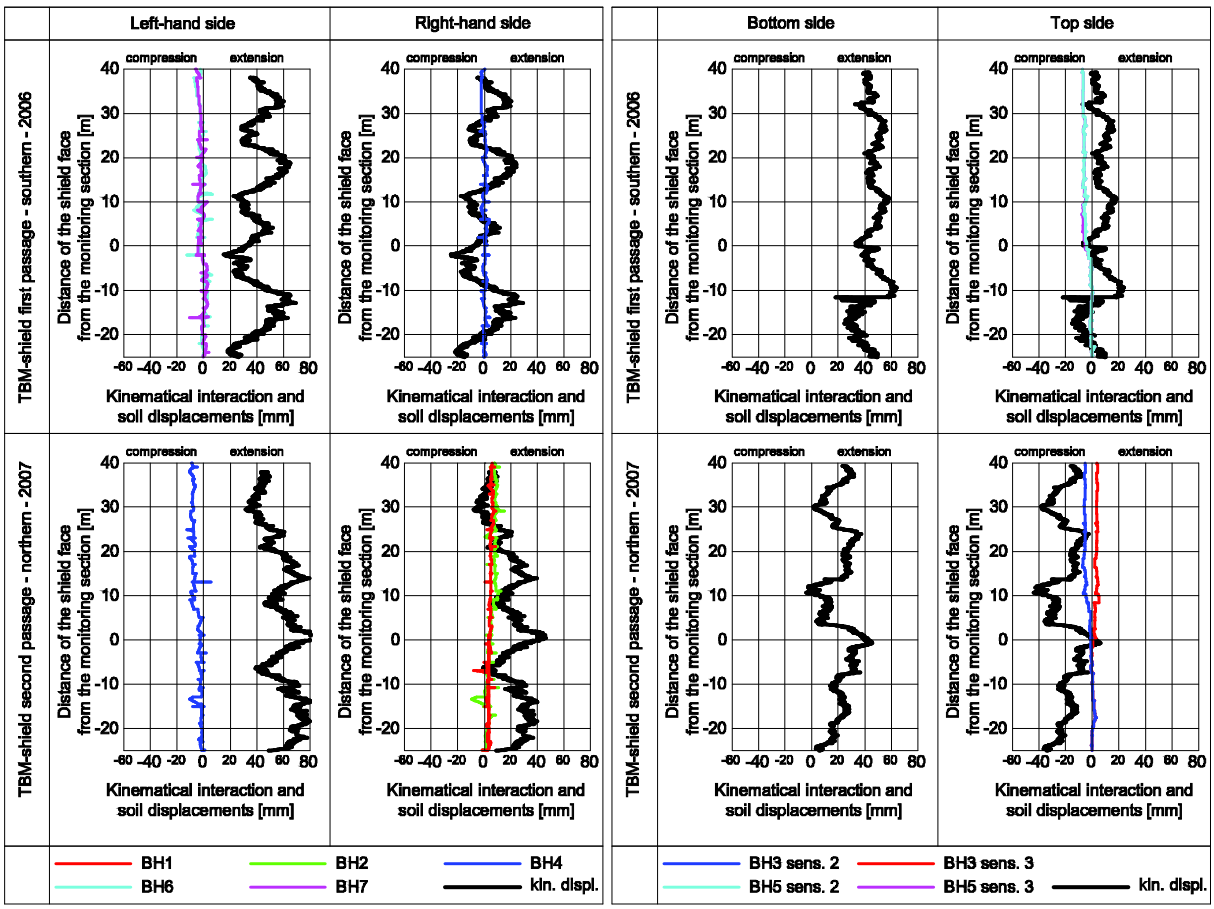

Figure 22. Shield-soil interaction and soil response – cross-section 4